ATTENUATION OF TRAVELING ACOUSTIC SHOCK WAVES IN TUBES

THEODORE C. BIELICKI
and
LAWRENCE RUSSELL, III

ATTENUATION OF TRAVELING ACOUSTIC SHOCK WAVES IN TUBES

* * * * *

Theodore C. Bielicki

and

Lawrence Russell, III

ATTENUATION OF TRAVELING ACOUSTIC SHOCK WAVES IN TUBES

by

Theodore C. Bielicki
Major, United States Army

and

Lawrence Russell, III
Captain, United States Army

Submitted in partial fulfillment of
the requirements for the degree of

MASTER OF SCIENCE
IN
PHYSICS

United States Naval Postgraduate School
Monterey, California

1 9 6 2

ATTENUATION OF TRAVELING ACOUSTIC SHOCK WAVES IN TUBES

by

Theodore C. Bielicki

and

Lawrence Russell, III

This work is accepted as fulfilling

the thesis requirement for the degree of

MASTER OF SCIENCE

IN

PHYSICS

from the

United States Naval Postgraduate School

ABSTRACT

The attenuation of fully developed, traveling, acoustic shock waves was studied with particular emphasis placed on obtaining reproducible results and extending the range of observation. High intensity sound waves produced by a siren were propagated in a 5.4 cm radius tube treated to eliminate reflection from the downstream end. After reaching a stable wave form the decay of the acoustic shock wave was measured over a distance of 4.5 m by means of a traveling microphone. The frequencies used were between 610 and 1130 cps resulting in a ratio of wavelength to tube radius of from 10 to 5. The pressure jump across the shock wave was from 1/35 to 1/8 atmosphere. Both of these ranges extend into previously uninvestigated regions.

A comprehensive analysis of 184 runs was made in order to compare the results to the empirical formula for the attenuation S as given by Medwin in his empirical formula. $S = S_{\infty} + 1/\delta$ const/f. Where S = .54 is the infinite plane wave attenuation, δ the shock strength, f the frequency, and const = 6.55 for our tube. Our results agree in that S = .50. However, the plots of S vs 1/f at constant $1/\delta$ varied from a straight line at frequencies above 900 cps. In addition plots of S vs $1/\delta$ at constant f show a small but decidedly negative slope.

The investigators wish to express their thanks to Prof. J.V. Sanders for his encouragement and continual guidance during the conduct of this investigation.

TABLE OF CONTENTS

LIST OF ILLUSTRATIONS

SYMBOLS AND DEFINITIONS

$\Delta p = P_2 - P_1$	Pressure jump
$\mathcal{E} = \Delta p / P_1$	Shock strength
$1/\mathcal{E} = P_1 / \Delta p$	Reciprocal shock strength
$S = \frac{d(1/\mathcal{E})}{d(x/\lambda)}$	Attenuation
λ = wavelength	Distance between successive shock fronts
f = frequency	Number of pressure pulses per second
R	Tube radius
c	Speed of propagation
γ	Ratio of specific heat at constant pressure to specific heat at constant volume
P_1	Pressure immediately before a shock
P_2	Pressure immediately after a shock
P_o	Pressure in medium when particle velocity equals zero
ρ_o	Density of medium when particle velocity equals zero

$$c_o = \sqrt{\frac{\gamma P_o}{\rho_o}}$$

I. INTRODUCTION

Finite amplitude sound waves, like pressure pulses of arbitrary wave form, are distorted as they progress through a gas. The portions of the wave of higher pressure are propagated at a greater velocity until the wave piles up at the front, forming a pressure discontinuity or shock pulse. It is well known that single shock pulse propagates at greater than the speed of sound due to its finite overpressure. However, when pressure pulses follow each other in rapid succession, as in a finite amplitude sound wave, each succeeding wave must propagate into the reduced pressure area of the one ahead of it, consequently the speed of a repeated shock wave is much less than that of a single shock, and is only slightly above the normal speed of sound. When the repeated shock waves have fully distorted to their characteristic N shape they propagate without further distortion except for attenuation.

The distortion and attenuation of these waves may be visualized as·

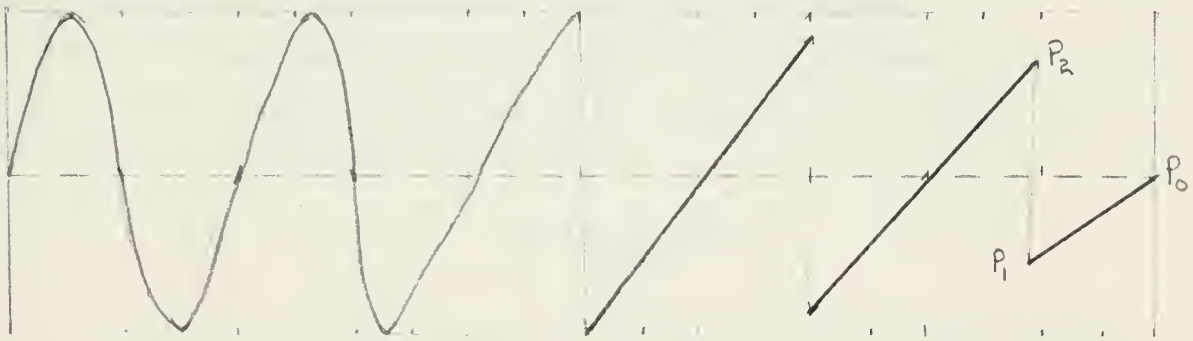

Fig. 1.

It may be noted that the attenuation is much greater after the pressure discontinuity has formed than before.

Previous investigations of the behavior of repeated plane shock waves in air in tubes include:

Rudnick[2], who studied pulses of up to 1/2 atmosphere propagated in a 10" diameter tube 60 feet long and ranging in frequency from 20 to 200 cps. He reports 35 traverses.

Werth[7], who used 1" and 1-1/2" dia tubes, measured frequencies from 300 to 1200 cps. His data is based on 46 traverses.

Wilson and Bies[4] had a 5" diameter tube and varied frequencies from 40 to 180 cps with an average pressure pulse of .1 atm. They reported 17 runs.

(The results of these three experiments agreed that it was very difficult to eliminate standing waves from the tubes, and that the estimated error was rather large. No dependence of attenuation per wave length on either frequency or tube radius was noted except by Werth, who had different average attenuations for his two different tubes.)

Anderson and Mehrtens[16] made 6 traverses in 3/4" and 1-1/2" tubes at about 500 to 700 cps, and discovered that there was possibly some frequency dependency of attenuation per wavelength and that attenuation increased with a decrease in tube radius.

Carpenter and Bauman[17] made 45 traverses at frequencies ranging from 450 to 925 cps in tubes having 2-1/4", 1-3/4", 1-1/4", and 3/4" diameters and having pressure pulses of about .1 atm. They again showed that there was a dependency of attenuation on both frequency and tube radius, but their data was too variable to enable them to say just what this dependency was, or to substantiate one particular theory over the others.

Medwin[6] then reported 12 more careful runs in a longer 3/4" diameter tube and made a thorough analysis of the previous data. This resulted in an empirical formula for attenuation

$$S = 0.54 + 1/\delta \frac{1.0 \times 10^{-3}}{R/\lambda} \quad .$$

A check of all previous data revealed that only the λ/R region of above 10 had been studied and that not much attempt was made to get repeated data at the same frequencies. Consequently the approach taken in the present investigation was to obtain data on many similar runs in a λ/R region below 10, where the tube effects should be smaller and the infinite plane wave effects of greater relative value. Six main frequencies were run in a 5.4 cm radius tube: 610, 725, 810, 950, 1050, and 1130. Attenuator pads were added at the upstream end of the traveling shock tube to extend the effective length of the tube, and to obtain data on attenuation in the less studied region of pressure pulses from 1/15 to 1/25 atm.

II. THEORY

The phenomenon of the initial distortion and formation of an N wave has been extensively investigated. One result of this investigation is the formula, derived by F.E. Fox and W.A. Wallace[8] based on the work of Earnshaw and Riemann, for the distance, L, required for the distorting wave to form a shock front.

$$L = N\lambda$$

$$\text{where } N = \left[\gamma/(\gamma+1)\pi^{-1}\left(\frac{\rho_o}{P_o}\right)\right]$$

which, evaluated for air as a perfect gas and a pressure pulse of .1 atm, gives 1.85 wavelengths.

As the attenuation of these pressure pulses is a decidedly non-linear effect, it has not lent itself to a thorough theoretical analysis. By following at least five different paths, three different conclusions have been reached by several investigators. The several different methods of approach have lead to four different theories to explain the attenuation of the plane infinite repeated shock wave, the three here and Medwin's empirical formula. Although arrived at by different paths, each of them agrees that the decrease in the value of the non-dimensional reciprocal pressure pulse per wavelength is constant, which we will call S_∞ . In our notation this is:

$$\frac{d(1/\delta)}{d(x/\lambda)} = \text{const}, S_\infty \qquad (1)$$

The different theories give S_∞ , in general, as follows:

Rudnick's[2] thermodynamic approach and Fay's earlier loss mechanism description as well as a hydrodynamic approach lead to the prediction that

$$S_\infty = \frac{\gamma+1}{2\gamma} .$$

Fay's[10] later energy surface propagation approach gives the formula

$$S_\infty = \frac{\gamma+1}{2\gamma} .$$

Westervelt[22] derived the formula $S_\infty = \frac{\gamma+1}{3\gamma}$.

The different theories give S_∞ for air as.

Rudnick	.86
Fay (later)	.57
Westervelt	.61
Medwin (empirical)	.54

In addition to the infinite plane wave attenuation, a term must be added to account for the attenuation due to the tube in which the measurements are made. Two formulas have been advanced describing this energy loss. Rudnick considered that the shock attenuation at the walls is made up of the Kirchoff infinitesimal attenuations of the Fourier sine wave components of the N wave. This led to the formula:

$$S_w = \frac{1.55}{R/f} \tag{2}$$

Medwin, on the other hand, by an analysis of the data available to him arrived at the empirical formula:

$$S_w = \frac{1.0 \times 10^{-3}}{R/\lambda} \tag{3}$$

It can be seen that these two theories agree that:

$$S_w = \frac{\text{const}}{R} \quad f^{n-1} \tag{4}$$

and differ in that:

	const.	n
Kirchoff-Rudnick	1.55	1/2
Medwin (empirical)	.353	0

The assumption is then generally made that the two effects are merely additive, giving the general formula for attenuation in acoustic shock waves in tubes as.

$$\frac{d(1/\delta)}{d(x/\lambda)} = S = S_\infty + \frac{1}{\delta} S_w \tag{5}$$

III EQUIPMENT

All measurements were made in a 5.4 cm radius seamless steel tube, which may be divided into four major functional segments as shown in Fig. 2. They are:

1. The generation section: The siren used (with the exponential horn and rotary chopper) was the same as used by Anderson and Mehrtens.[16] However, the armature and field circuits of the .5 HP Dumore Motor were modified as shown in Fig. 3. Improved operation resulted from this circuit, especially in obtaining higher and more consistant frequencies. With switch "A" in the "extra speed" position, switch "B" closed, and switch "C" in the "start" then "run" position, the batteries B1 (in series with the generator) permitted a smoother operation of motor, making it less sensitive to generator fluctuations and affording a higher potential. Resistors R1 and R2, and Ammeters A1 and A2, permitted fine adjustments of the current in the field and the armature. The batteries were kept at a constant full charge by recharging between runs by placing switch "A" in the "Run and Charge" position, switches "B" and "C" open, and switches "D" and "E" closed. The flexibility to run without batteries B1 in the circuit was retained by throwing switch "A" in the "Run and Charge" position while in operation (i.e., switches B and C closed and switches D and E open).

Improvement in the flexibility and control of air flow from the compressor to siren was made by moving the compressor away from the immediate vicinty of siren and siren motor (affording easy access for maintenance purposes) and by running compressed air through a panel with controls and gauges: air flow selector (high and low) and air flow meter, pressure controller, and thermometer.

2. Shock wave development section: A section of tube 56" long was added to the upstream end, ahead of the cable traverse, to provide a distance for the N waves to form before any measurements were taken. This distance, in addition to that already built into the apparatus, was found to be sufficient for the waves with frequency above 400 cps to become steady when the compressor was delivering maximum flow.

The added advantage of having a tube separation available at a point downstream from the region of shock development and upstream from the measuring instruments was that it permitted the insertion of attenuators of various

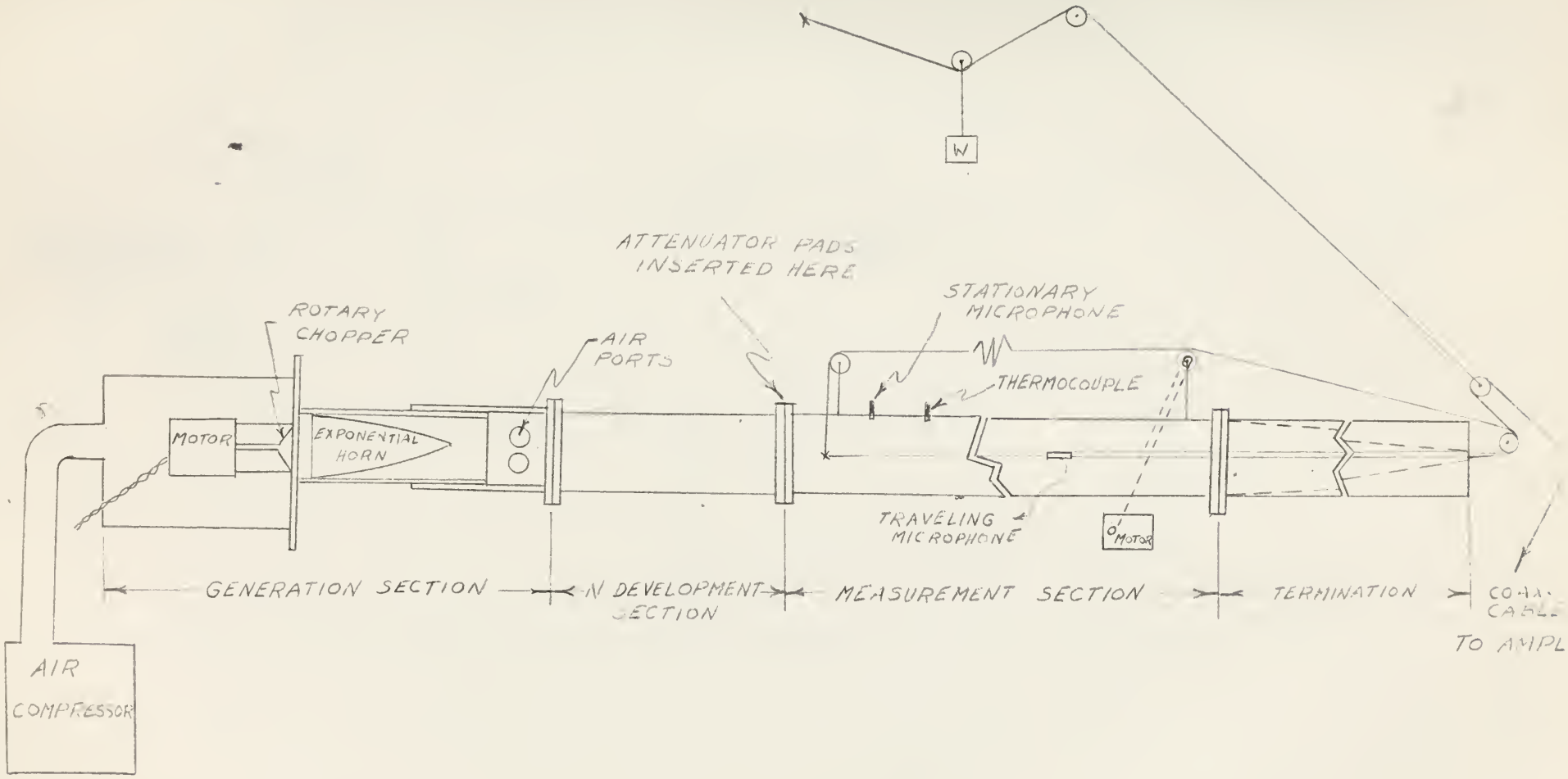

FIGURE 2. SCHEMATIC DIAGRAM OF EQUIPMENT

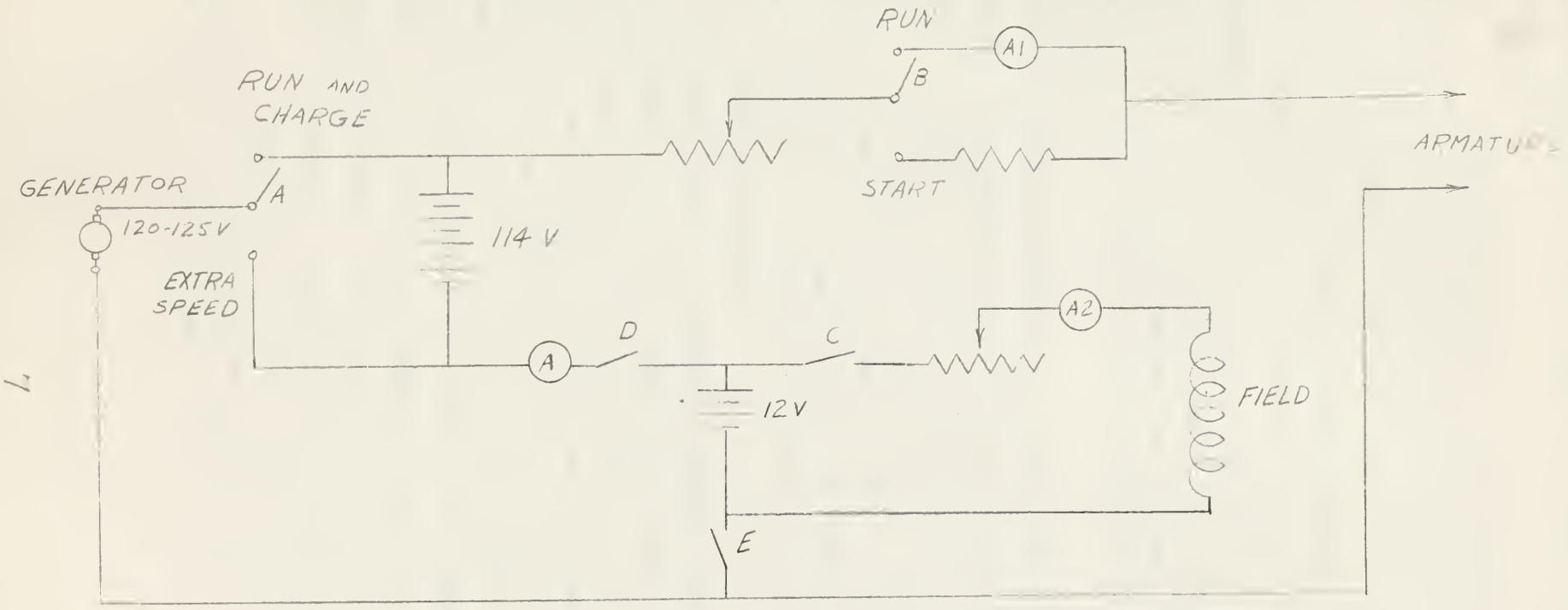

FIGURE 3. MODIFIED FIELD AND ARMATURE CIRCUITS FOR ACCURATE CONTROL OF FREQUENCY

thickness (glass wool) which reduced the shock strength, achieving larger values of $1/\delta$.

3. Measurement section: The microphones used were 3 mm diameter x 3.4 mm long hollow cylindrical crystals of barium titanate. Two such barium titanate microphones were used: one traveling on a stainless steel cable centered inside the tube and driven at a constant speed by an electric motor, while the other microphone was mounted in the wall of the tube at a fixed location. The stationary microphone facilitated the physical measurement of wavelength. A duel trace Tektronic Oscilloscope Type 545 was attached to the two microphones, and the traveling microphone was stopped each time the traces coincided and the distance traveled afforded a good measurement against which to check wavelength as determined by means outlined in the Appendix.

The traveling microphone had a flat response to above 100 kc and was calibrated by comparison with a previously accurately calibrated barium titanate microphone to deliver a signal of 353 mv per atmosphere of pressure swing. It was attached to a teflon shielded coaxial cable (Microdot #93-3620) to minimize noise pick up. Since the teflon covering is brittle and cannot make a sharp turn, the small pulley (1/4" radius) at the end of the microphone traverse was replaced by a larger pulley (1" radius) at the end of the tube beyond the termination.

The signal from the traveling microphone was connected, after amplification, directly into a VTVM (which reads proportional to the average full-wave rectified voltage) and a CRO (used to monitor the wave form and check the peak to peak voltages obtained from the other meters), as shown in Fig. 4. The signal was then filtered so that only the fundamental frequency component was passed, and this sine wave was used as the signal for the recorder. Several independent checks were made on the linearity of the recorder trace obtained in this manner with respect to the input signal (Figs. 5 and 6) and it was amply verified. The filtered sine wave was also amplified and connected to a frequency counter which determined the frequency.

4. Termination section: Glass wool padding of increasing thickness was used in the six foot long termination section to absorb the traveling shock waves. It was also found that by running the steel carrying cable as

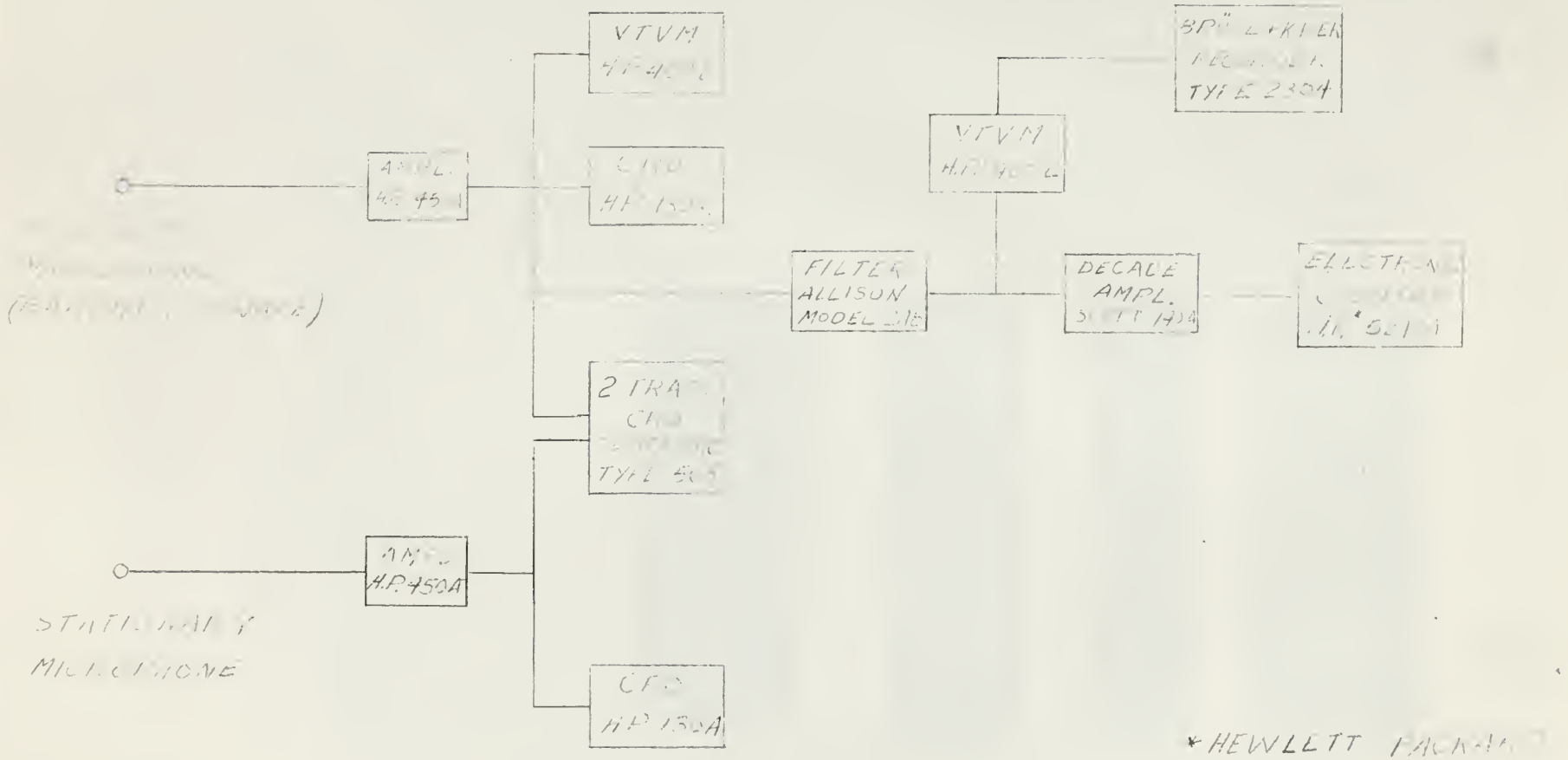

FIGURE 4. BLOCK DIAGRAM OF ELECTRIC CIRCUITS

a.

b.

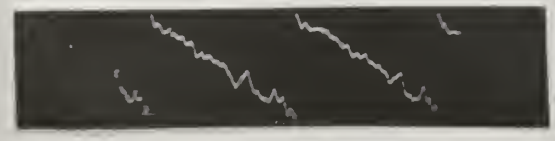

c.

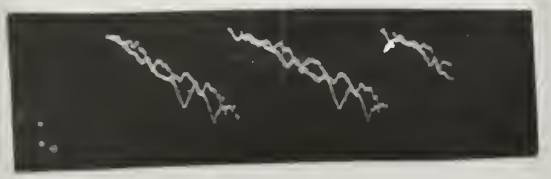

d.

Figure 5. Shock waves photographed during linearity check of recorder at intervals along tube [taken at correspondingly numbered locations on Figure 6] portray their progressive attenuation.

a. Point 1, shock equals 41.8 mv [nearest to source].
b. Point 2, 37.3 mv.
c. Points 3 and 4, 29.8 and 28.7 mv, respectively. Relative voltages discernable against CRO scale.
d. Point 5, 21.6 mv.

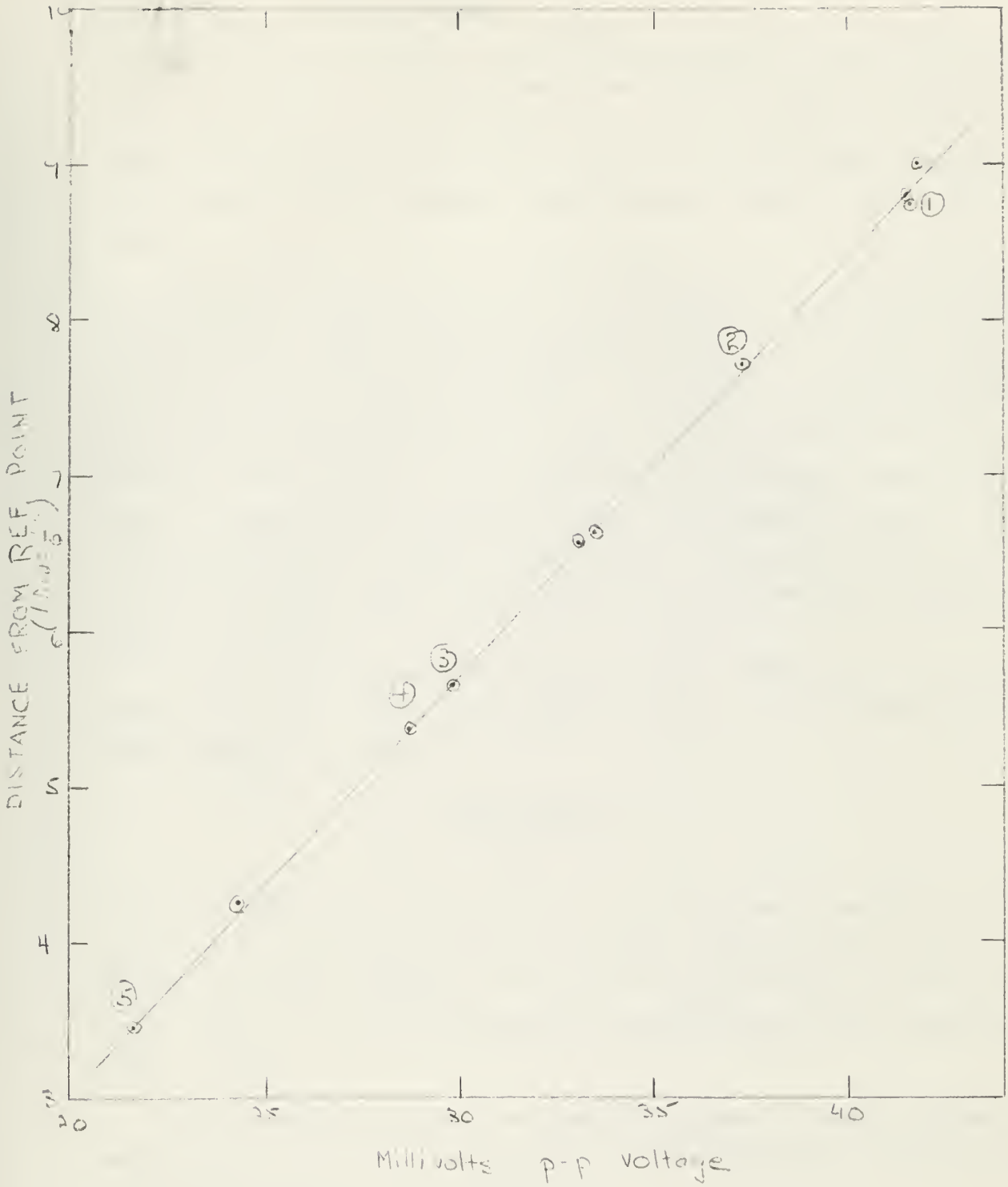

FIGURE 6. LINEARITY CHECK OF RECORDER

IV. CONDUCT OF THE EXPERIMENT

At selected frequencies, the traveling microphone was traversed the length of the tube (5 meters) starting at a point nearest the siren (provided a good shock wave was formed at the limit of traverse at that end). VTVM and CRO readings were made at each end and the microphone traversed back toward the siren, giving a typical recorder trace as shown in Figs. 7,8 and 9.

Runs were made only after the CRO indicated that a stable wave form had been attained. In many cases this meant that only a portion of the traverse length could be used, as the microphone had to be moved to where there was good shock before starting to record. It was noted on several discarded traces that the attenuation of a not quite developed shock wave was noticeably less than that for a fully developed one, consequently great care was taken to measure only the N wave portion. The attached pictures of CRO traces show what is a "good" and "not quite" N wave, with a picture of the attenuated signal at the other end of the tube included for comparison (Figs. 10 and 11).

The recorder traces were analyzed by first determining the voltages at regular intervals. These peak to peak voltages were determined from the VTVM readings, and computed as:

$$V_{pp} = \frac{\text{VTVM reading}}{1.1} \times 4$$

since the VTVM read the rms value of a pure sine wave, but indicated proportional to the average rectified voltage[16]. Dividing by 1.1 gave the average full wave rectified voltage which for an N wave is 1/4 the peak to peak voltage. Since the microphone delivered 353 mv per atm pressure swing, $\Delta p = V_{pp}/353$.

The atmospheric pressure was used as P_o, since a better absolute reference pressure could not be determined and this should be the average pressure in the tube. Since $1/\delta$ is defined as

$$\frac{P_1}{P_2 - P_1}, \text{ and } P_o = \frac{P_1 + P_2}{2}: \quad 1/\delta = \frac{P_o}{P_2 - P_1} - 1/2 = \frac{P_o}{\Delta p} - 1/2.$$

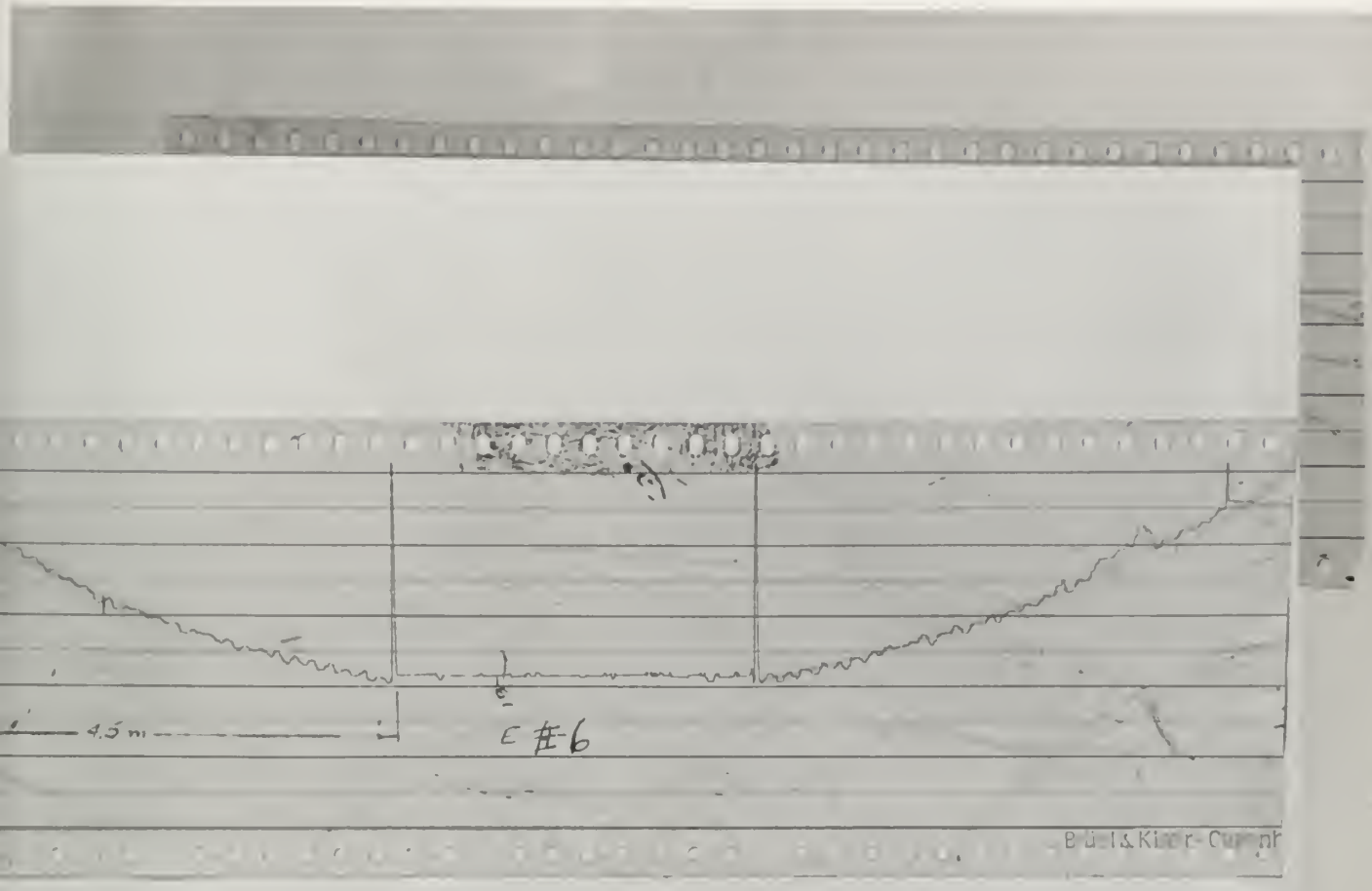

Figure 7. A typical recorder trace for a frequency of 1050 cps. Note the comparatively large amount of attenuation of the primary pulses and the reflected wave [as indicated by the standing wave envelope]. The pressure jump is .1 atm at the high end and .055 atm at the low end of the tube. Also notice the effect of transient noise on the right hand trace.

These traces have a linear vertical dependency on voltage, with the exact scale determined for each set of runs as described in the text.

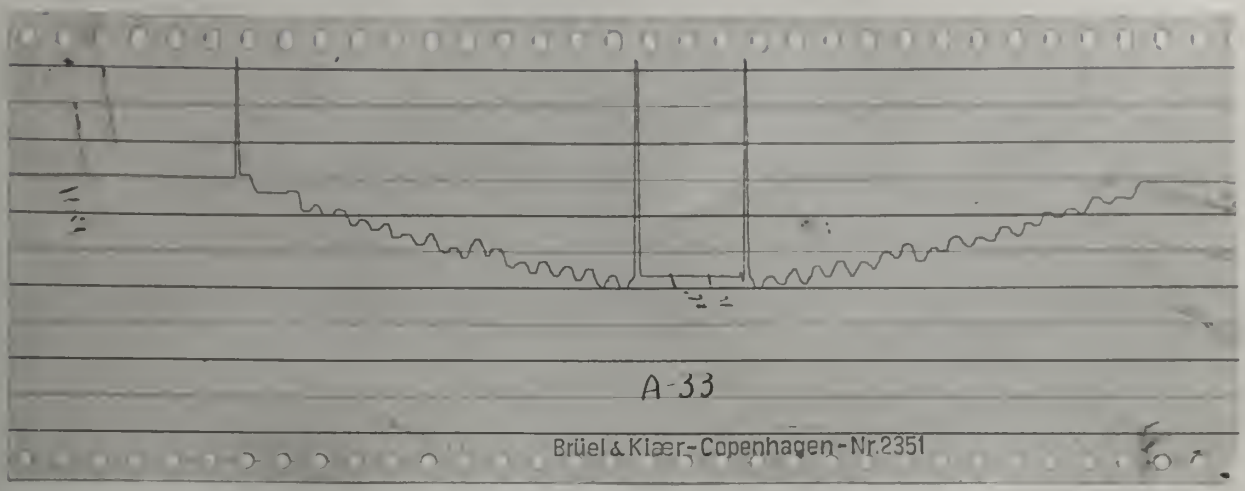

Figure 8. A recorder trace for 810 cps with the same input pressure. This trace shows an attenuation from a .1 atm to a .063 atm pressure pulse.

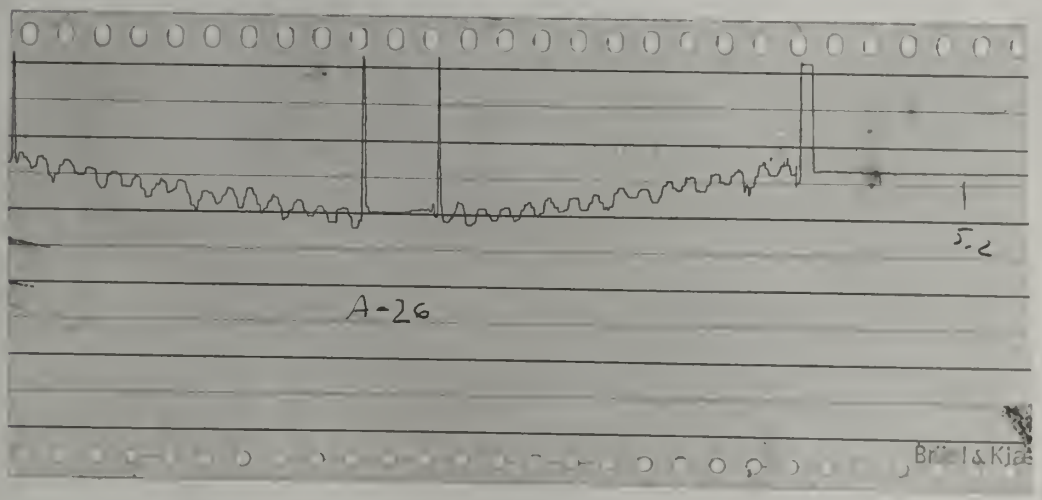

Figure 9. A recorder trace for 810 cps with a lower input pressure. This shows attenuation from .053 atm to .043 atm. Note: The spikes at the start and end of each traverse are marked automatically as the carriage activates a switch at each end.

Figure 10. A Partial Shock Wave Formation. The peaks have not quite caught up with the shock front.

a.

b.

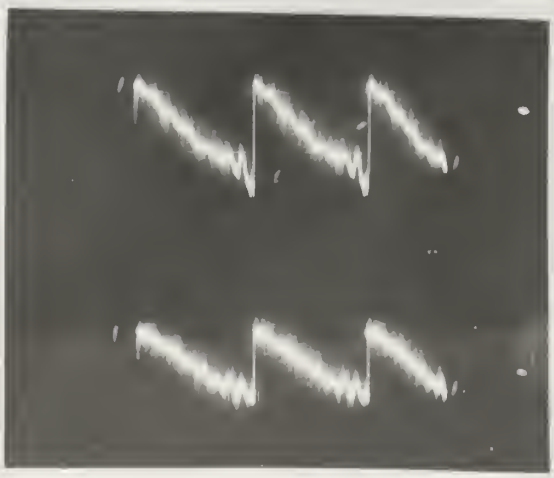

Figure 11. A fully formed shock wave [N wave]:
a. at maximum peak-to-peak amplitude,
b. attenuated as it proceeds down the tube,
[greater attenuation evident at greater distance from source].

These values of $1/\delta$ were plotted vs distance to obtain the curves for the individual runs.

A total of 422 runs was made and recorded. After the first 230 runs, the data were processed and the reduction of S with increased $1/\delta$ was noted. A thorough recheck of instruments, methods, and microphones was made and 192 additional runs were made. Results of data obtained in this second group were similar to that obtained in the initial group. This report is based on 184 runs out of the second group of runs made as indicated above.

Several collateral investigations were performed (See Appendix). They include: the influence of filters on matching a tube to a source, the attenuation of standing waves, wave length, propagation speed and temperature measurements, and attenuator pads for increasing the effective length of the tube.

V. RESULTS

a. $1/\delta$ vs x/λ Graphs

The recorder traces obtained were analyzed to determine voltage vs distance. These voltages were then used to calculate $1/\delta$ values and the results for each run plotted as an individual $1/\delta$ vs x graph.

All the graphs for runs taken on the same day, at the same frequency, and in the same $1/\delta$ region were then correlated by picking some value of $1/\delta$ as a base point that was common to all of them. Values of $1/\delta$ at various wavelengths away from that point were measured and tabulated. Then these values of $1/\delta$ were averaged to obtain the points for that set of runs.

The points for sets of runs in different $1/\delta$ regions were then aligned so that the composite would represent the attenuation in a longer tube than any individual run could. Fig. 12 to 17 are plots of these average values.

In some instances data were taken in the same $1/\delta$ region at the same frequency on different days, consequently some of the graphs have more than one set of points in the same region of $1/\delta$. The total number of runs averaged to obtain each data point is indicated on the graphs.

Early in this investigation it was noted that the slope of the $1/\delta$ vs x/λ curves diminished rather than increased with an increase in the value of $1/\delta$. This was in direct conflict with the effect noted by Prof. Medwin. Careful re-analysis of all data and rejection of all that showed the presence of appreciable noise failed to eliminate, or even greatly reduce, this effect. It was felt that possibly, since the area of investigation was in the region of λ/R of 5 to 10, a region previously not investigated, the reduction in wall effects, and consequent relative increase in importance of the plane wave effects may have caused a previously masked phenomenon to become apparent. Another alternative was a high steady noise level.

It was noted in some of the later runs, when the noise level of the siren was higher, the measured attenuation was noticeably less. For the $1/\delta$ region of 9 - 15, two separate sets of runs at 950 cps were compared, one with an average S of .679 and another with an S of .63. It was found that an increase in the noise level between the two sets of runs of only 1 mv peak to peak signal would have caused this deviation. As there was more noise apparent in the low S runs, this was probably a cause of the difference. Most of the noise is believed to be due to unsteadiness of the siren, but some may have been caused in the tube as well as by electronic pick-up.

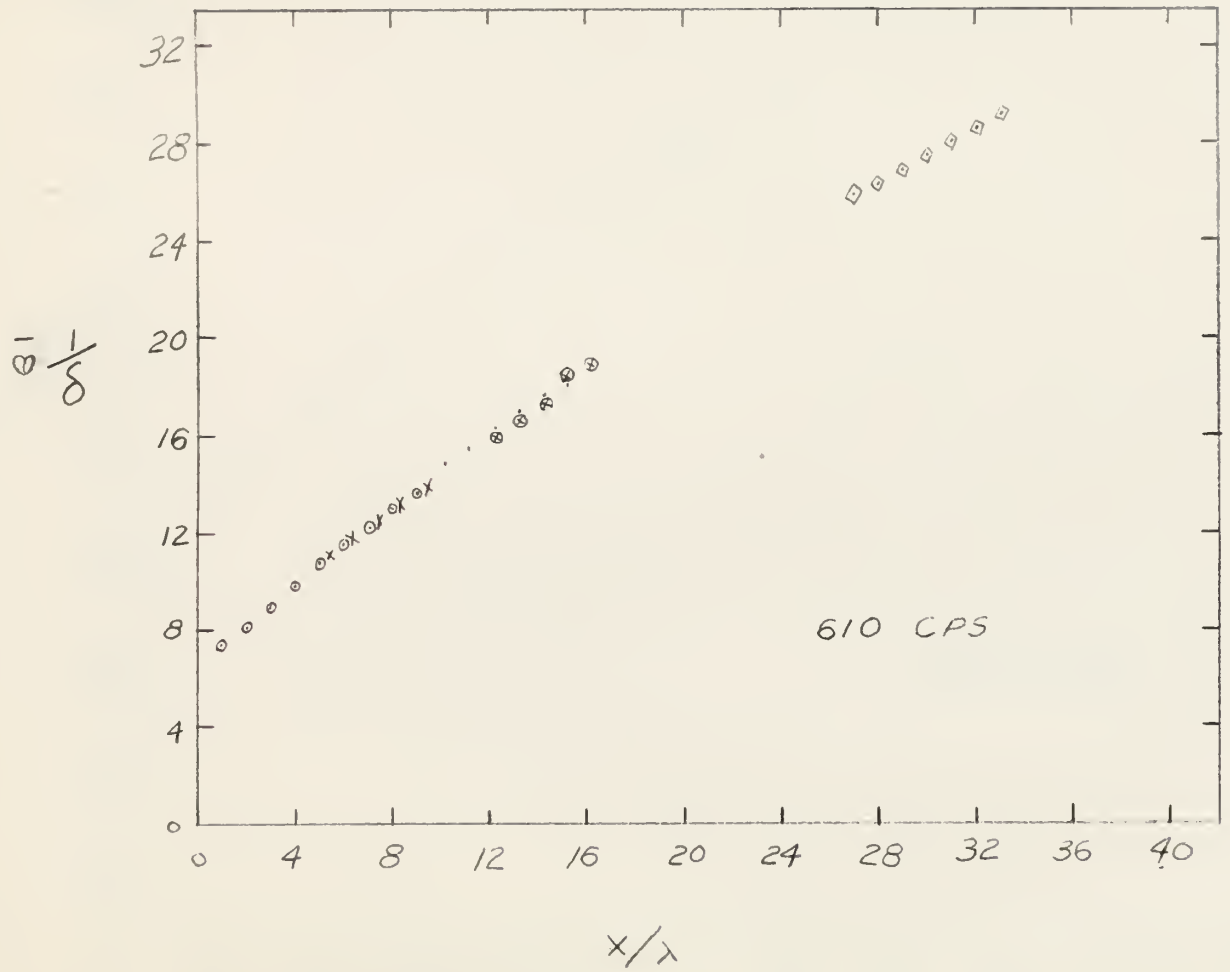

FIGURE 12

⊙ 5 RUNS
× 15 RUNS
⊗ 8 RUNS
. 4 RUNS
⊡ 3 RUNS

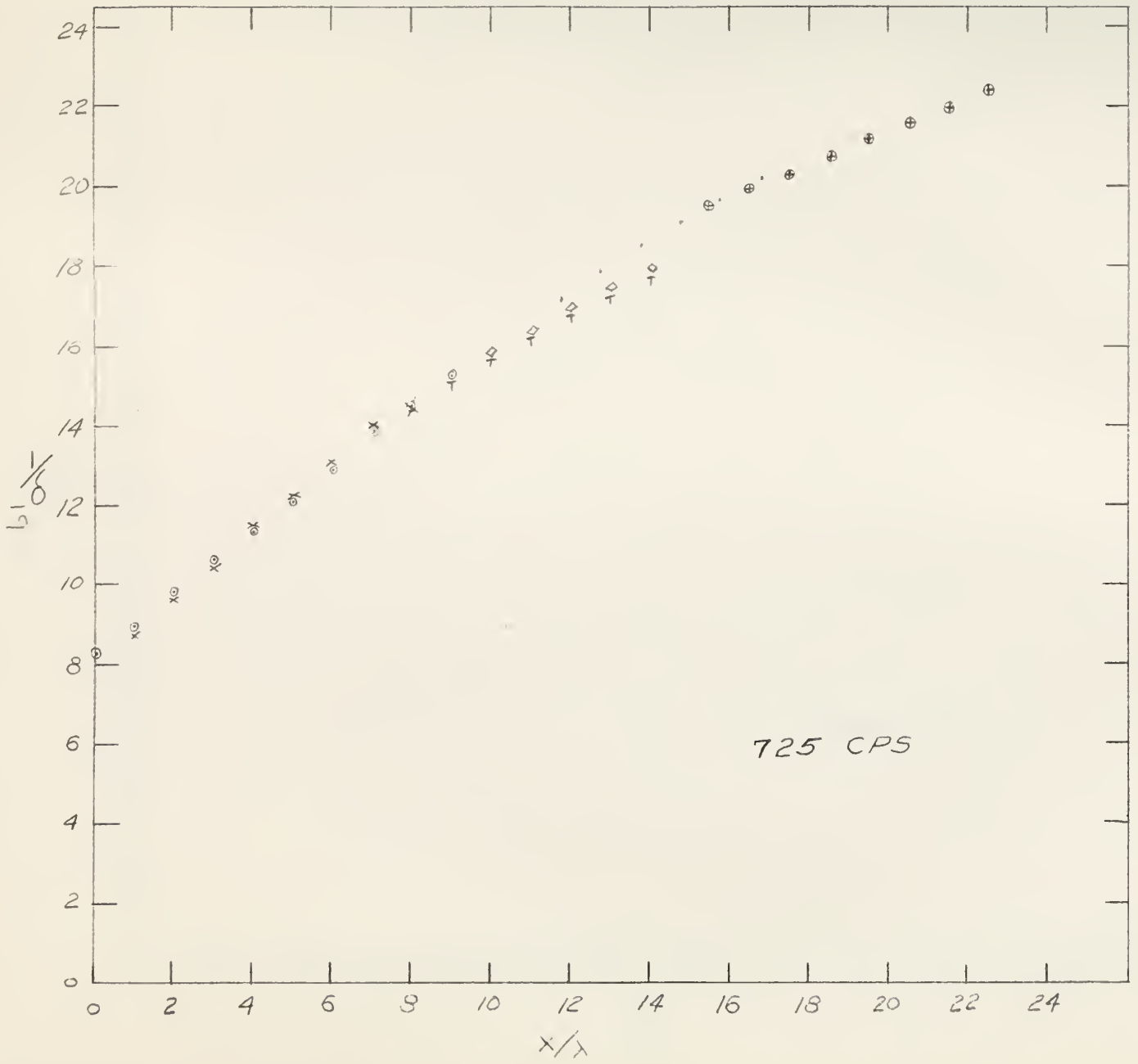

FIGURE 13

⊙ 11 RUNS
× 4 RUNS
◇ 4 RUNS
T 10 RUNS
· 8 RUNS
⊕ 3 RUNS

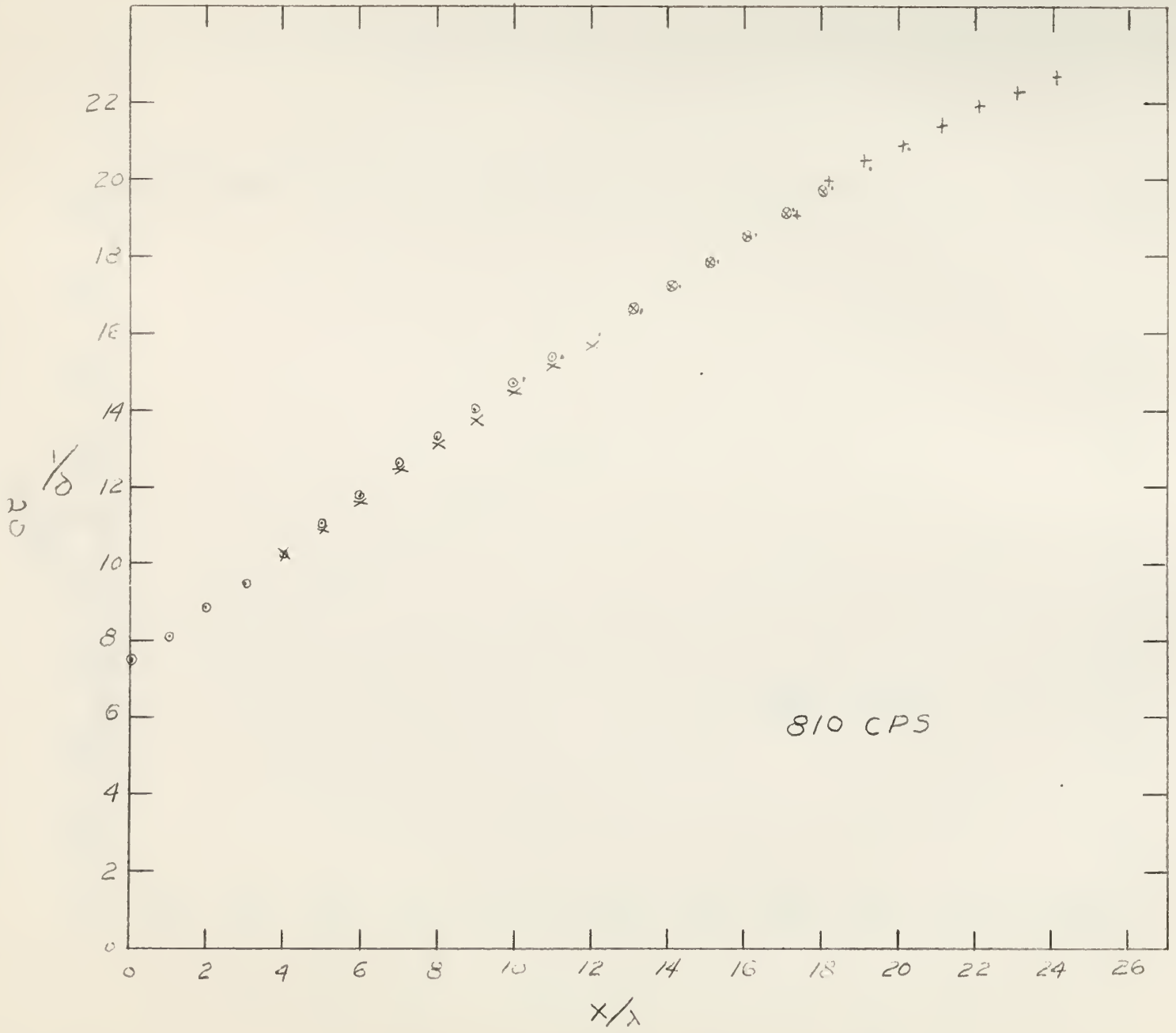

FIGURE 14

⊙ 12 RUNS
x 6 RUNS
. 8 RUNS
⊗ 8 RUNS
+ 5 RUNS

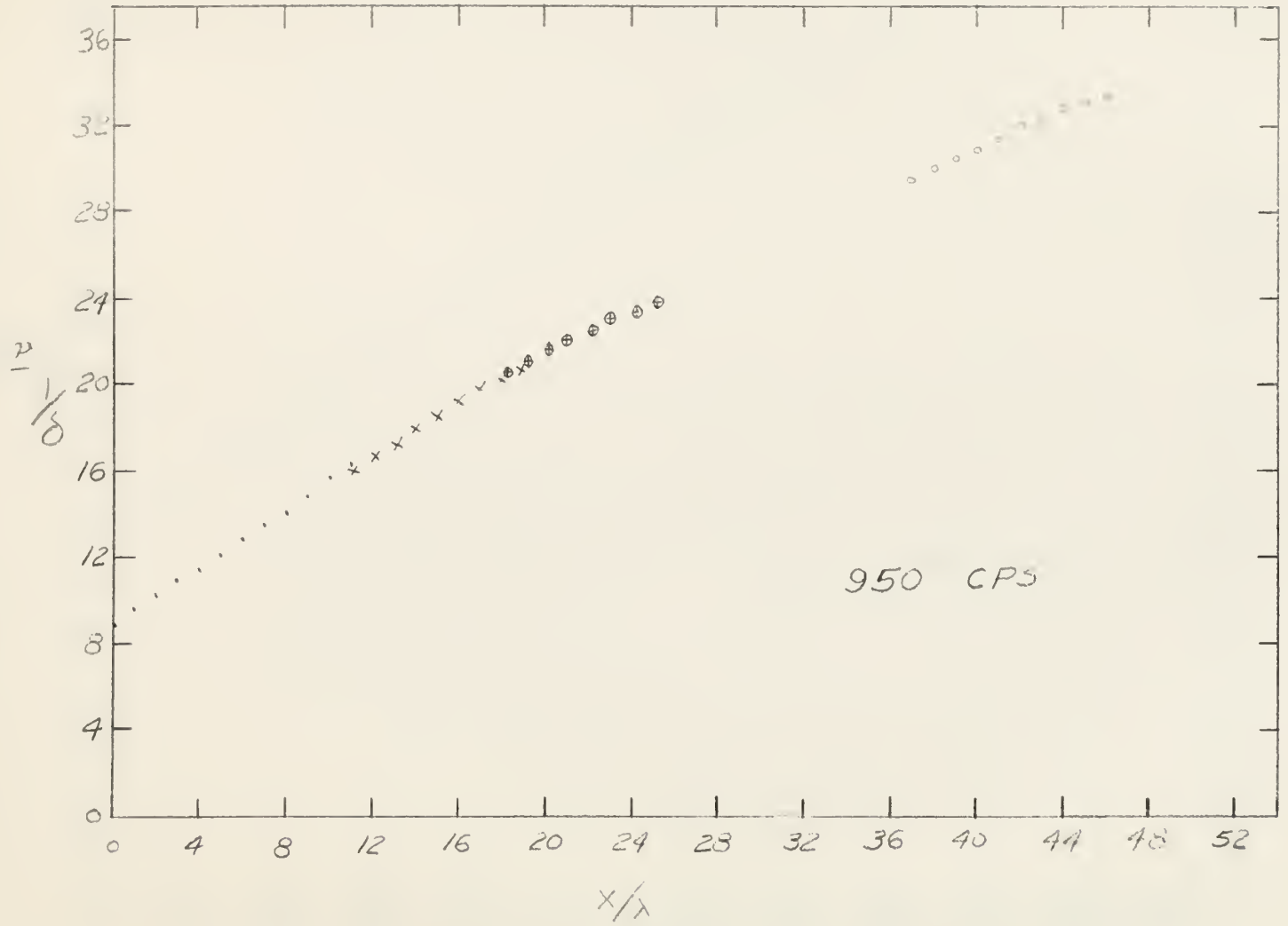

FIGURE 15

· 17 RUNS

× 8 RUNS

⊕ 12 RUNS

○ 8 RUNS

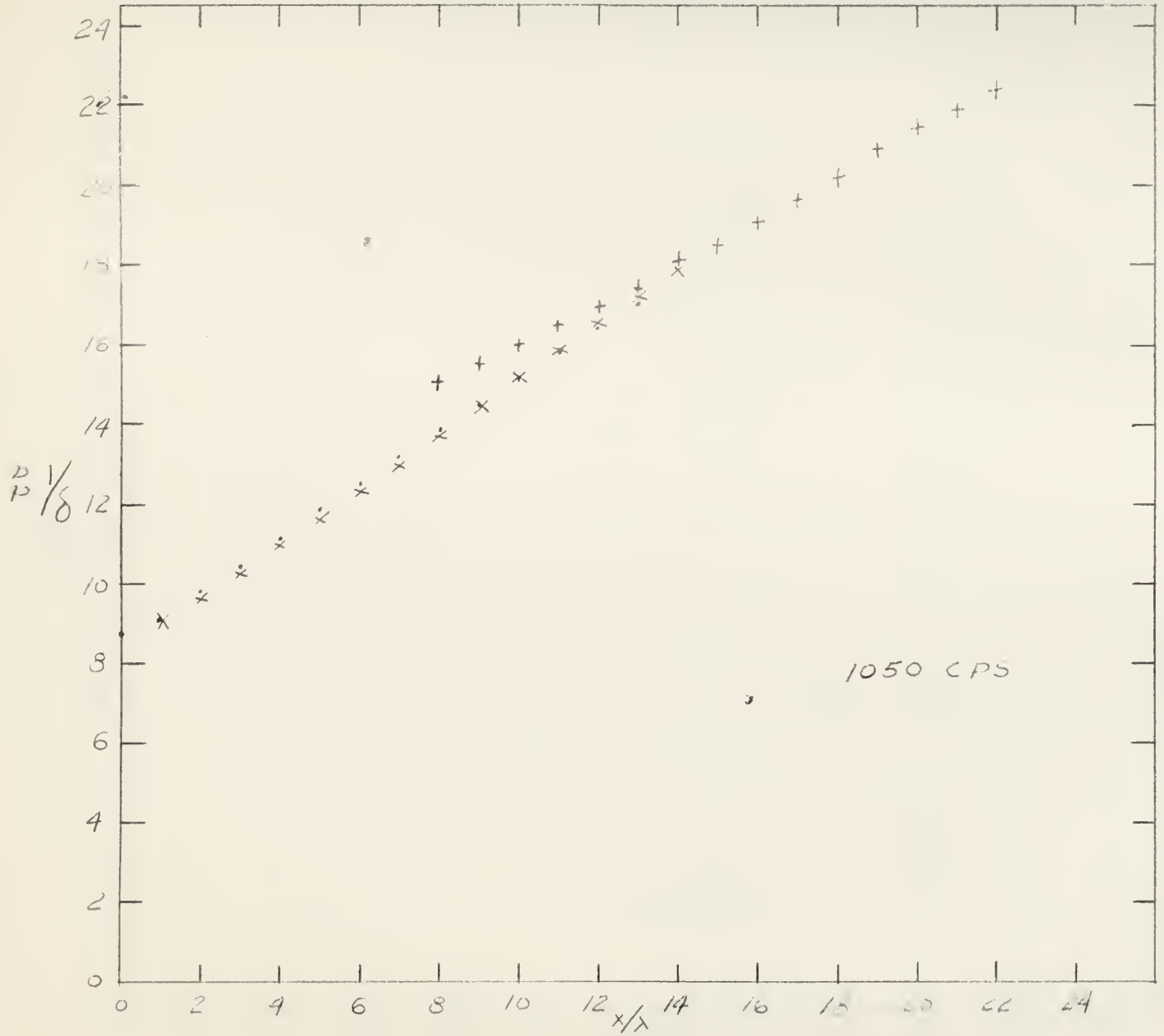

FIGURE 16

. 3 RUNS
x 4 RUNS
+ 4 RUNS

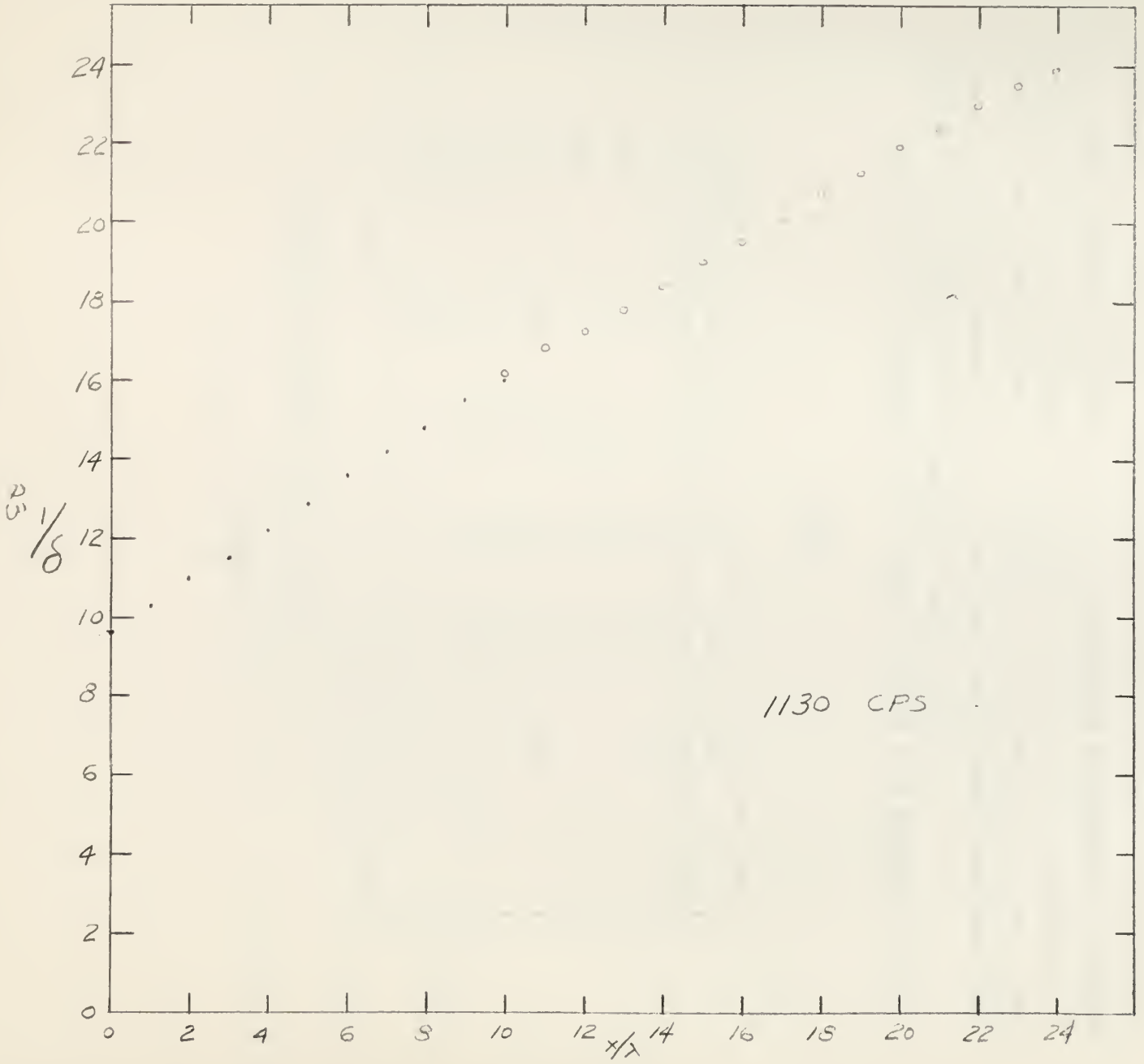

FIGURE 17

• 7 RUNS

○ 4 RUNS

b. Frequency dependence of S_w

The four different theories on the attenuation of plane acoustic shock waves are seen to vary only in the predicted slope of the $1/\delta$ vs x/λ curve. Each of these anticipates a linear relationship, with deviations from a straight line being attributed to wall effects. As our measurements were made in a tube with a λ/R ratio of from 10.25 to 5.6, and previous investigations were generally in the λ/R range of 20 and higher, it was anticipated that a much smaller wall effect would be observed.

It is also a consequence of these theories that S_∞ is independent of frequency. If this is so, any variation of the attenuation with frequency in a given diameter tube must be due to the effects introduced by the tube. Since the greatest influence that the tube can have on the attenuation is probably due to wall effects, an analysis of the behavior of repeated shock waves of varying frequencies in a given tube should reveal much about the dependence of shock wave attenuation on wall effects.

Values of S at different $1/\delta$'s were obtained from Figures 12 to 17.

TABLE

f \ 1/8	10	14	19	23	31
610 cps	.81	.75	.69	.65	.43
725	.78	.73	.64	.42	
810	.73	.70	.62	.43	
950	.68	.66	.58	.50	.41
1050	.70	.70	.60	.51	
1130	.67	.63	.59	.55	
1000	.68				

Combining equations 4 and 5 gives:

$$S = S_\infty + 1/\delta \ \frac{\text{const}}{R} \ f^{n-1} .$$

The values of S determined for different frequencies at the same value of $1/\delta$ plotted against various powers of the frequency should give a straight line when the proper power is used.

Figs. 18 thru 20 are plots of our data with n = - 1/2, 0, and 1/2. Fig. 21 is the 3/4" tube data of Prof. Medwin and students and Fig. 22 is 10" tube data of I. Rudnick, both plotted for n = 0.

A quick check of larger values of n showed difinitely no correlation, but smaller values were generally well fitted up to and including n = - 3. It was also noted that the lower the value assigned to n, the higher was the intercept with the y axis. This intercept should be S_∞ .

The values of S_∞ and S_w predicted by the various formulas are indicated on the graphs for n equals 1/2 (as predicted by the classical formula) and n equals 0 (as postulated by Prof. Medwin).

Also, it may be noted that the formula predicts that the slope of the best straight line should be the constant $\frac{ac}{R\delta}$, thus giving a means of determining "a" and the functional dependence on $1/\delta$. Our data of Fig. 19 for the $1/\delta$ region of 19 has a slope that would give a value of "a" of .02, which is in close agreement with the "a" for a $1/\delta$ of 20 of 0.02 ($20 \times 1.0 \times 10^{-3}$) (Equation 3). However our data indicates that "a" is not a constant. This data fits well the empirical equation $a/\delta = (b - d/\delta)$ with b = 0.047 and d = 0.0015.

To further confirm the value of n, another plot was attempted: Since

$$S - S_\infty = \frac{ac}{\delta R} f^{n-1}$$

$$\log (S - S_\infty) = \log \frac{ac}{\delta R} + (n - 1) \log f$$

This plot is very dependent on the value of S_∞ subtracted from the gross slope, and seems to be of value mainly in determining this parameter. Figs. 23 and 24 show this plot with n = 0 and various values of S_∞ .

Fig. 25 shows 3/4" dia tube data of Medwin, Carpenter and Bauman, and Anderson and Mehrtens plotted with S_∞ = .54 and S_∞ = .50.

Fig. 26 shows 10" dia Soundrive data plotted with S_∞ = .54 and S_∞ = .50.

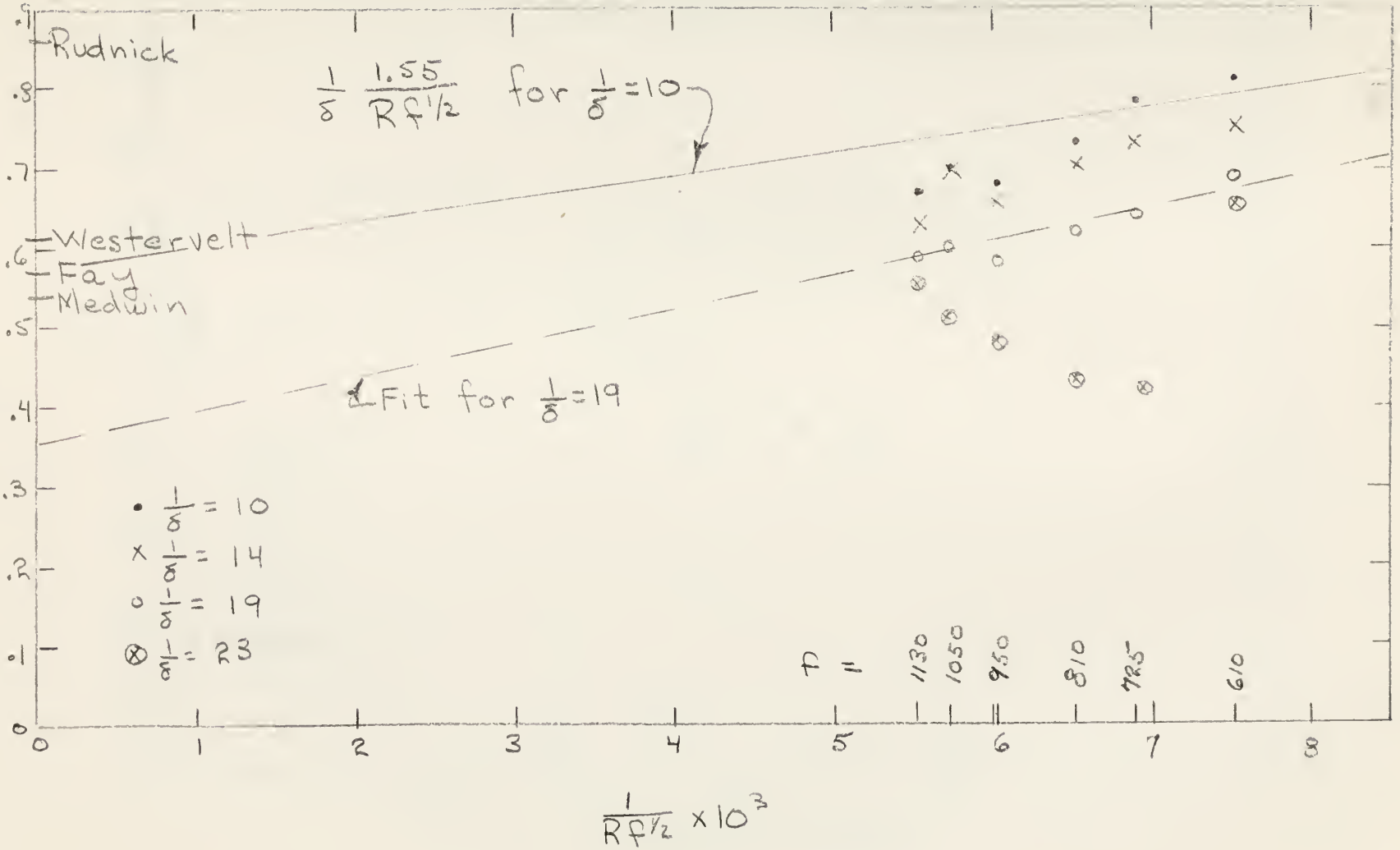

Figure 18
n = ½ Plot

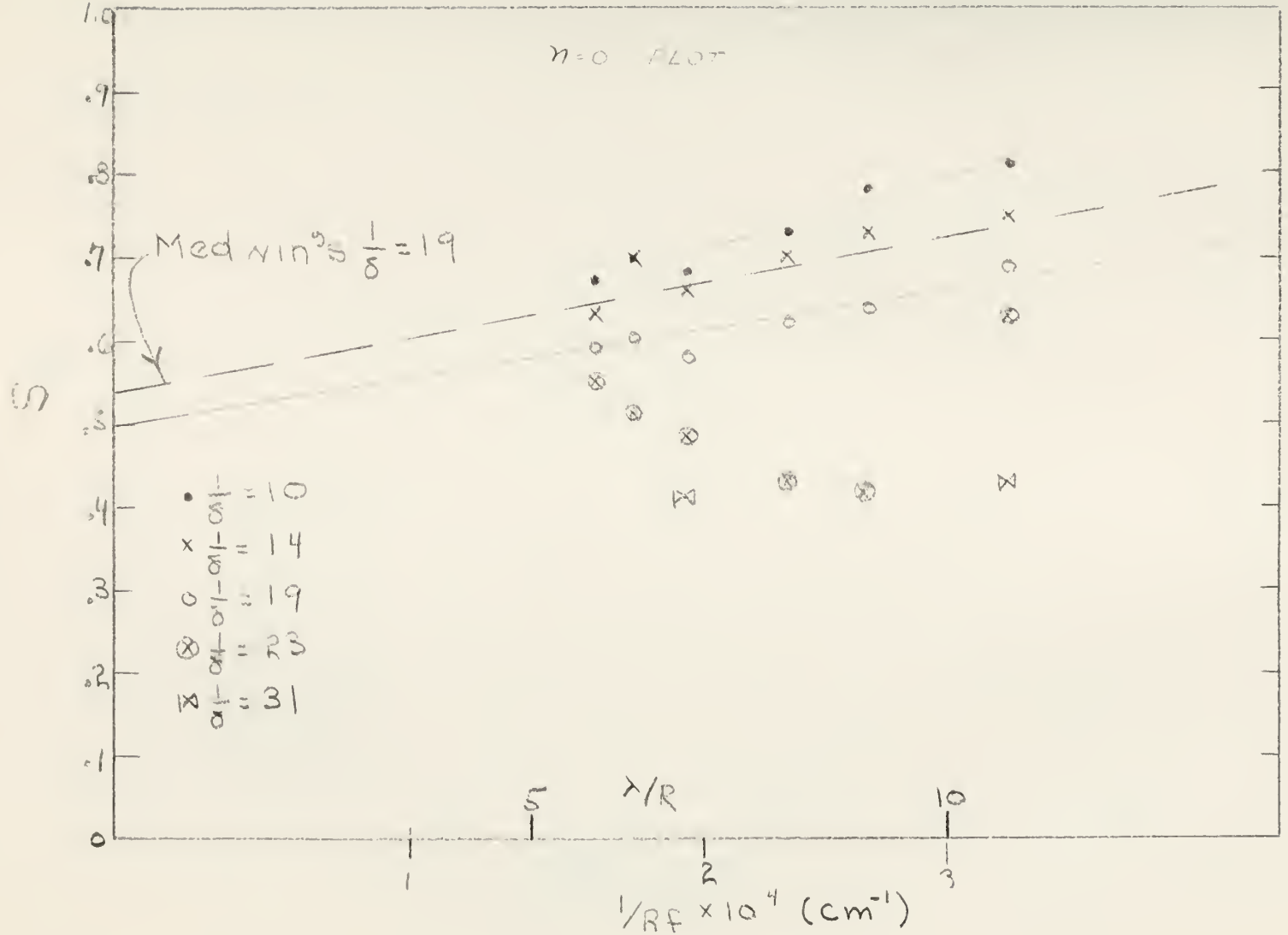
n=0 PLOT
Med min $\frac{1}{\delta}$ = 19
$\frac{1}{\delta}$
1.0
.9
.8
.7
.6
.5
.4
.3
.2
.1
0
• $\frac{1}{\delta}$ = 10
× $\frac{1}{\delta}$ = 14
○ $\frac{1}{\delta}$ = 19
⊗ $\frac{1}{\delta}$ = 23
⊠ $\frac{1}{\delta}$ = 31
λ/R
5
10
1
2
3
1/Rf × 10⁴ (cm⁻¹)

FIGURE 11

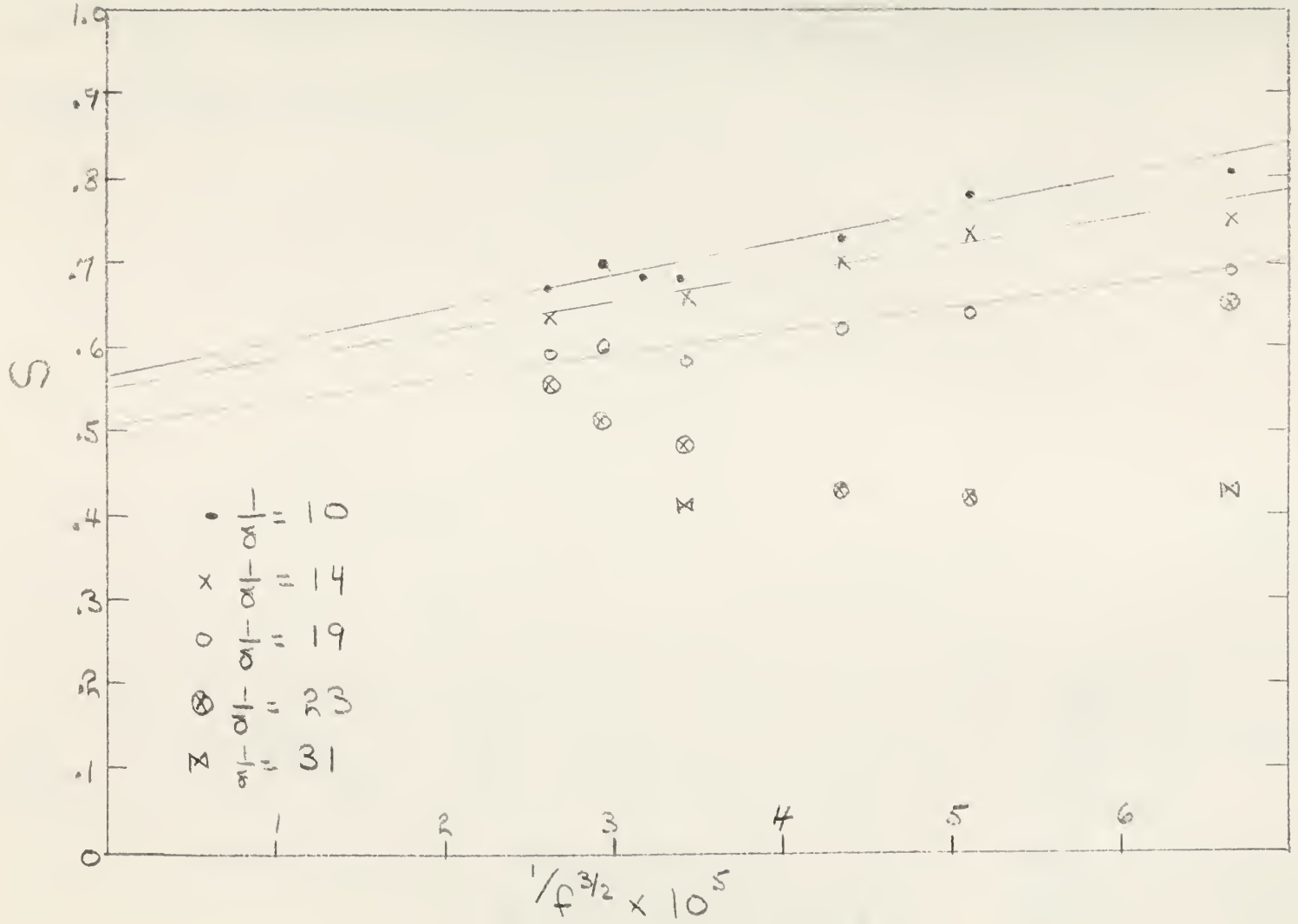

FIGURE 20
$n = -1/2$ Plot

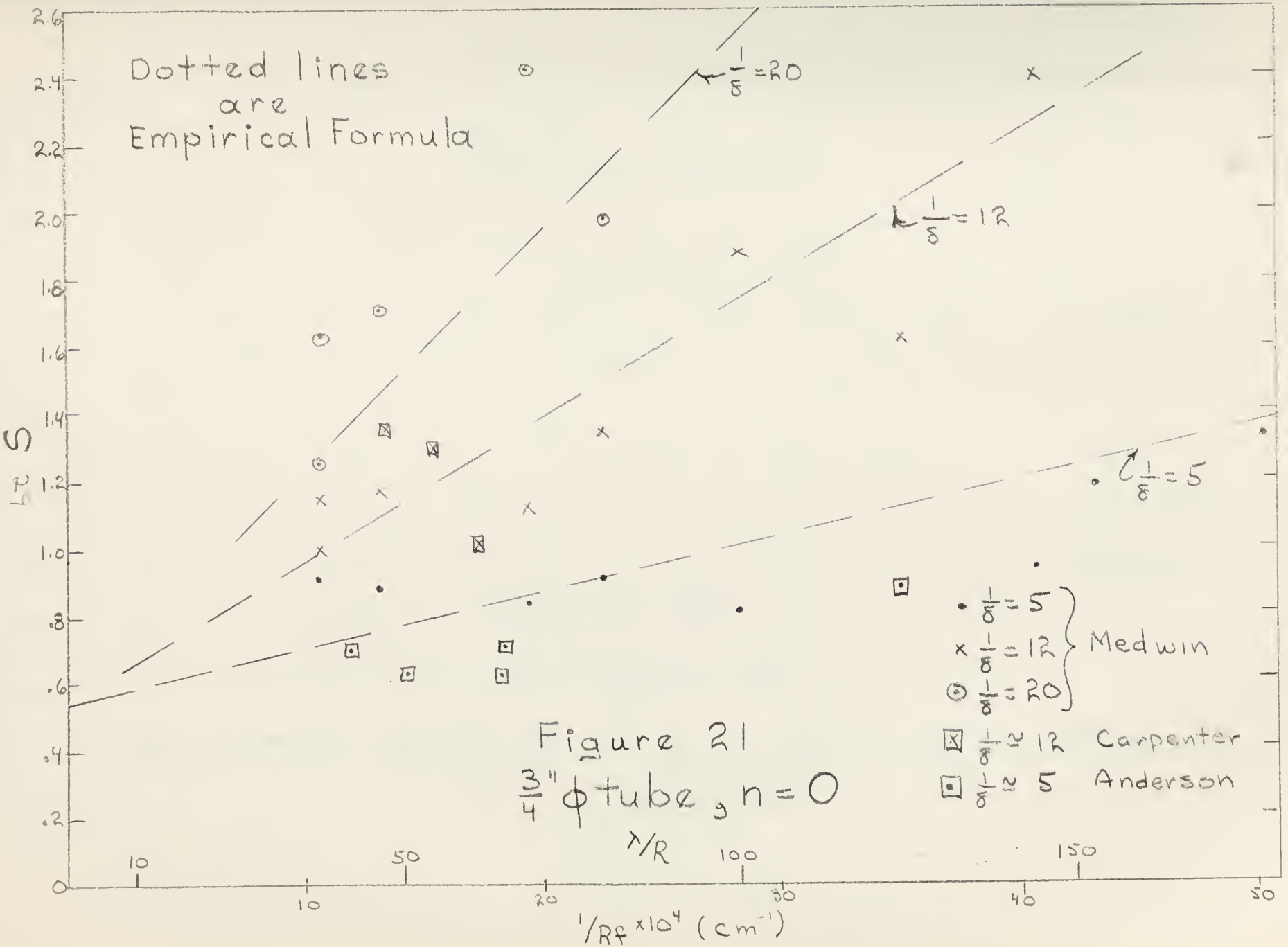

Figure 21

$\frac{3}{4}$" ϕ tube, $n=0$

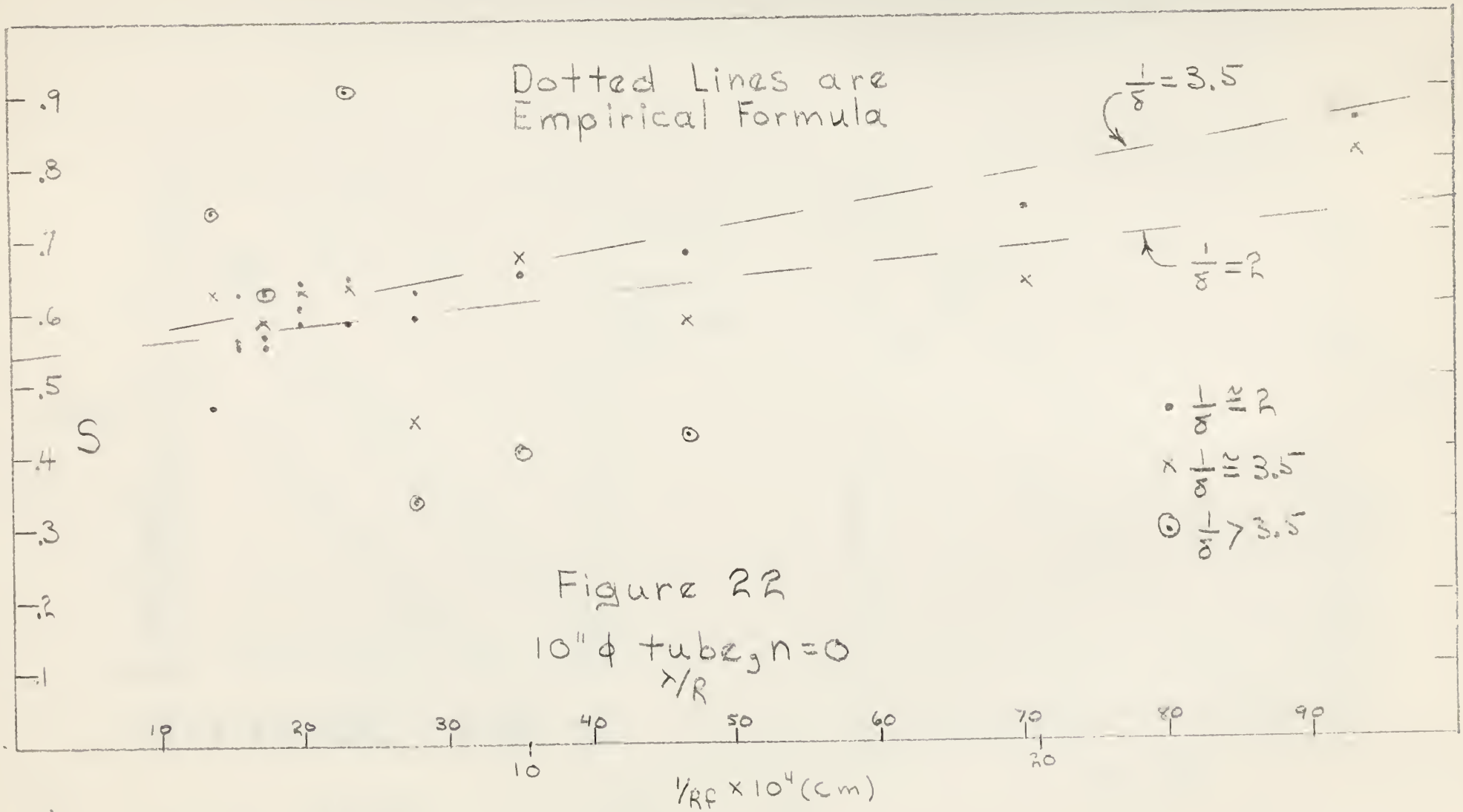

Figure 22

10" ϕ tube, n=0

x/R

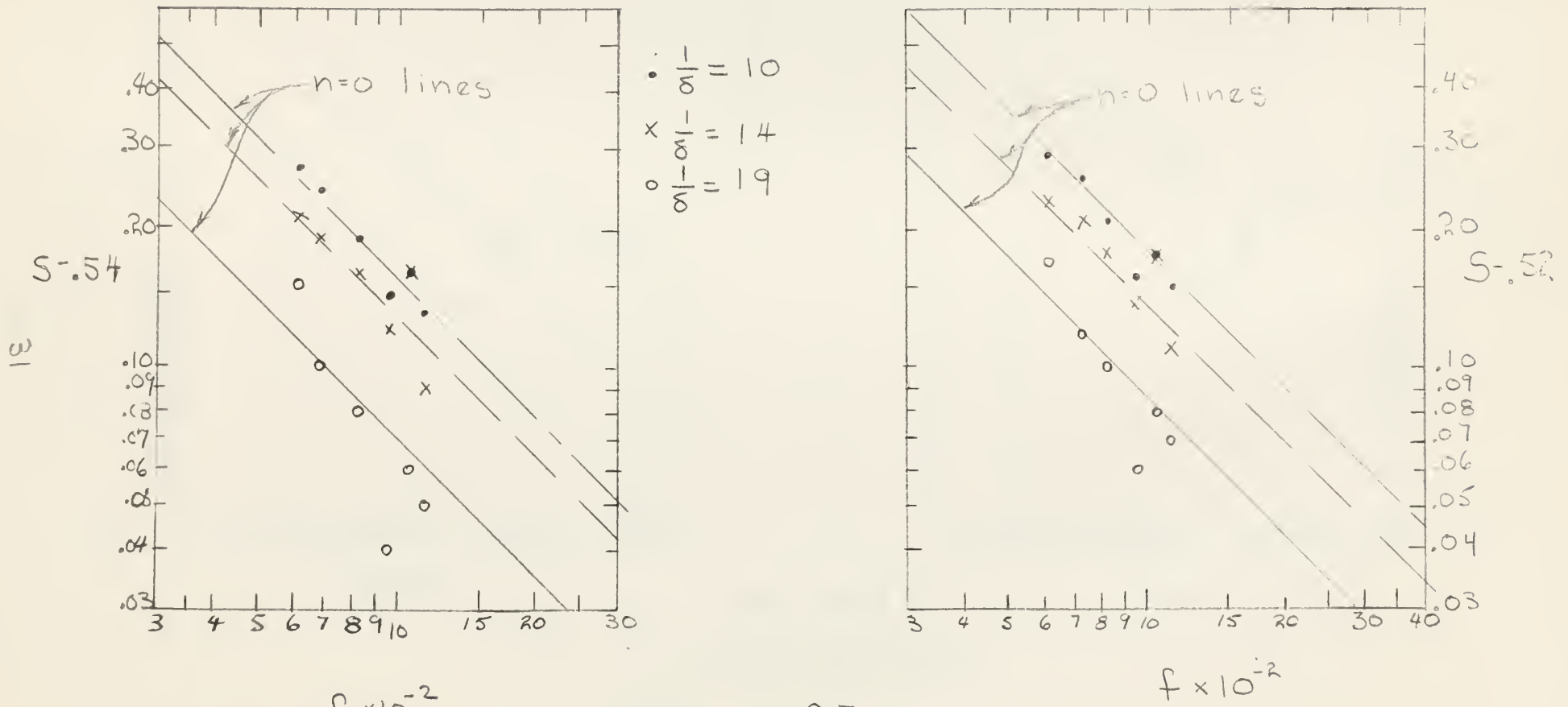

Figure 23
5.4 cm R tube

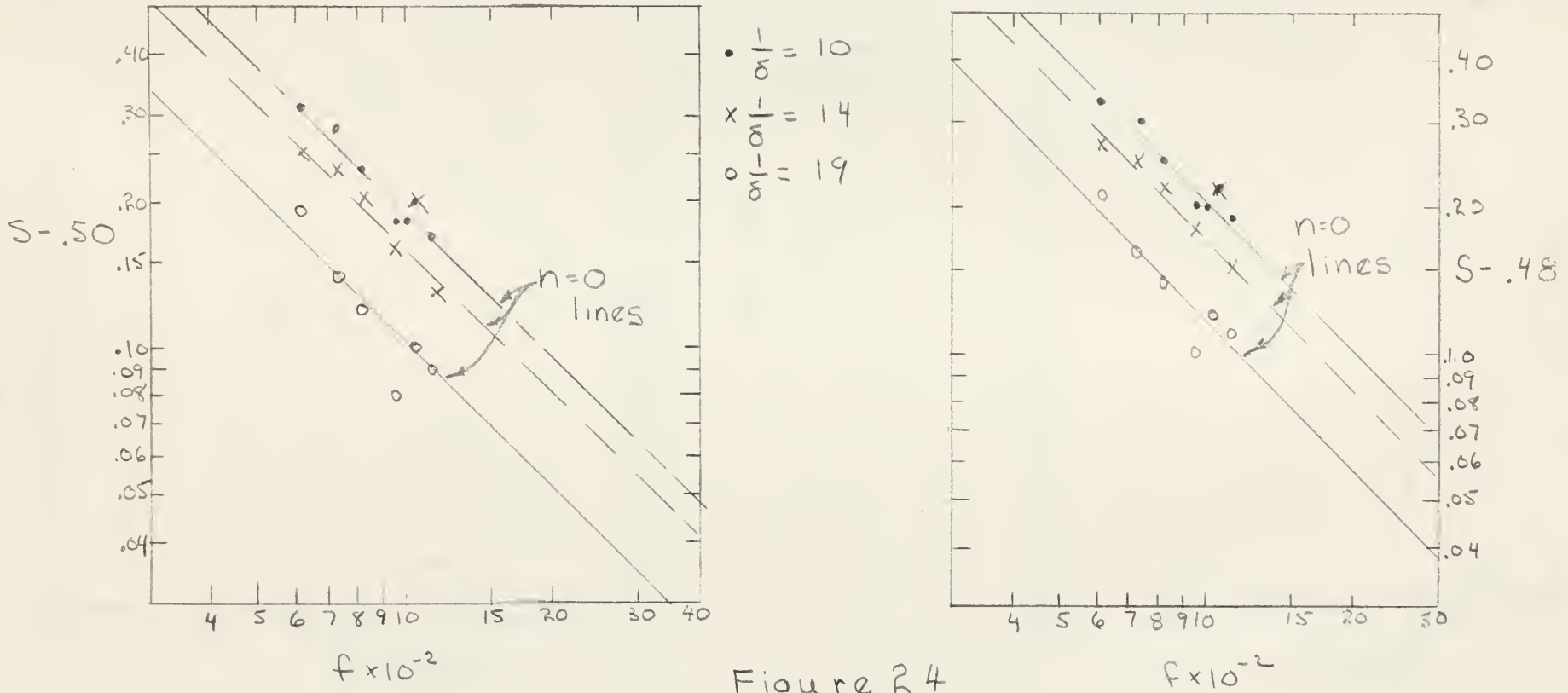

Figure 24

5.4 cm R tube

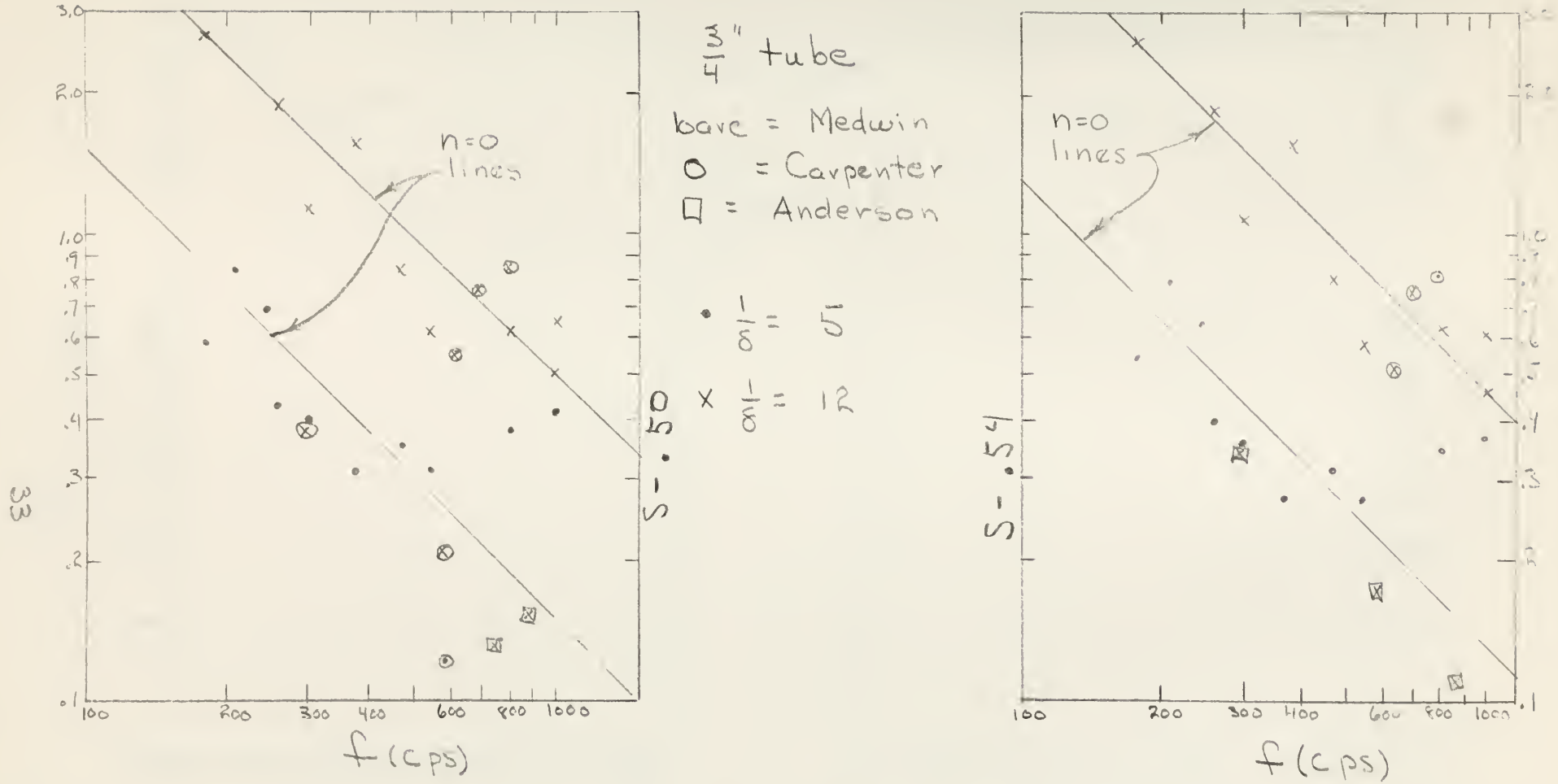

Figure 25
.95 cm R tube

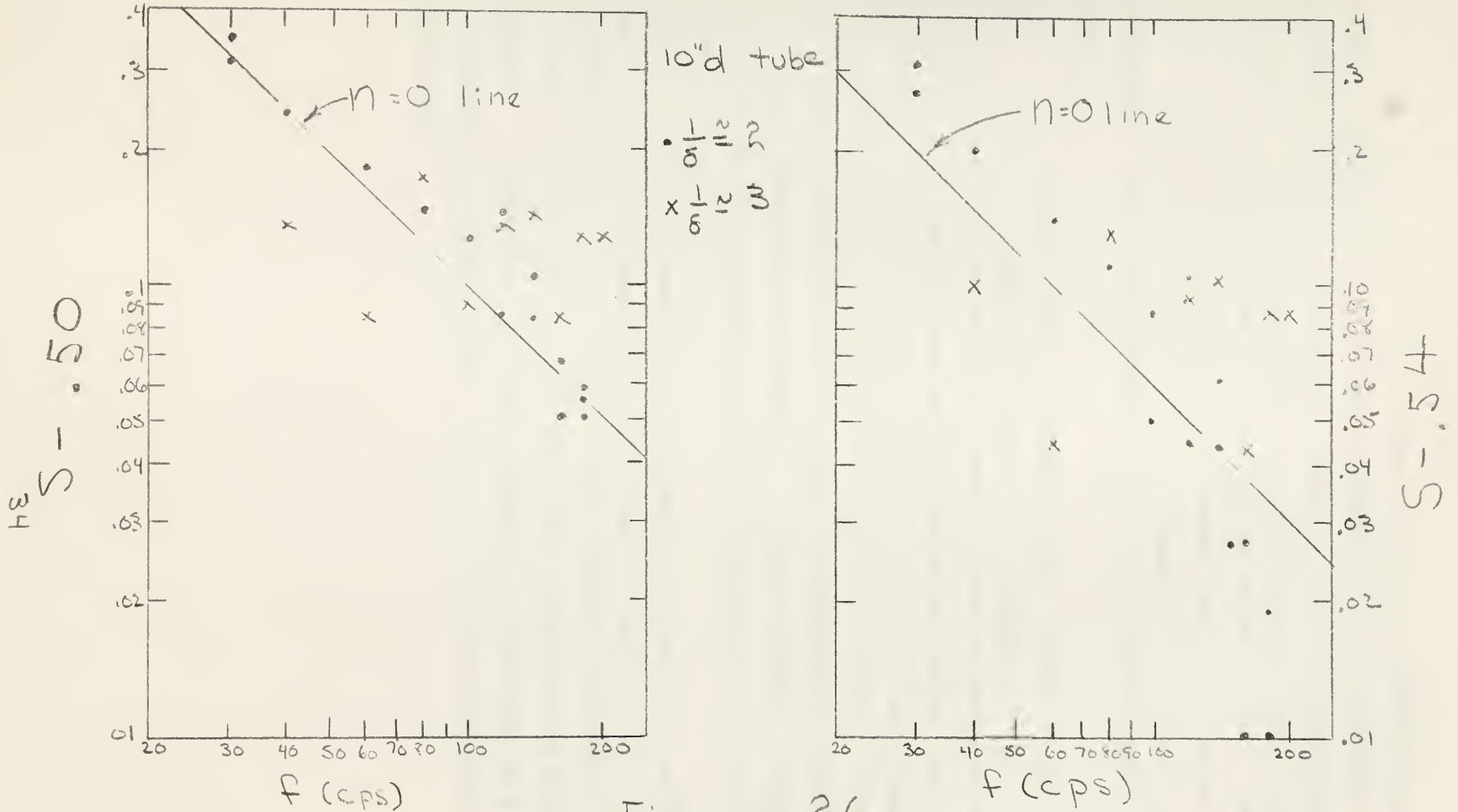

Figure 26

12.7 cm R tube

Soundrive Report Data

c. Frequency dependence of S_∞ .

A rather unexpected effect was noted at frequencies above 900 cps. As can be seen from Fig. 27, the attenuation does not continue to decrease with an increase in frequency, but seems to turn about and increase with frequency. A re-check of the 3/4" dia tube data also showed signs of this increase but there it makes itself apparent below 800 cps. This effect was also noted by Anderson and Mehrtens, based, however, on rather limited data.

In Fig. 27, the behavior of the attenuation is shown as a function of frequency. Each curve represents data for the same $1/\delta$ and in one diameter tube.

It is postulated that this effect could be caused in one of two ways:

(1) The onset of turbulent flow throughout the tube. It is anticipated that the flow behind the shock is turbulent when the pressure jump is large. At lower frequencies these shocks are farther apart, so the turbulence can die out between shocks. At some critical frequency, the turbulence will not have died out by the time the next shock arrives, thus this shock is propagating into a greatly disarrayed medium and should have its energy dissipated more swiftly. A further increase in frequency should increase the disarrangement of the gas immediately in front of the shock and thus increase attenuation.

(2) The presence of cross modes. For our tube for the frequencies above 900 cps the wavelength of the 2^d and 3^d harmonics is no longer large compared to the radius. At some critical frequency depending on the tube radius, this may cause a change in the wall attenuation of the higher harmonics, and consequently in the attenuation of the N wave as a whole. It is estimated that at about 2000 cps, when $\lambda = 17.7$ cm, these cross modes may be propagated.

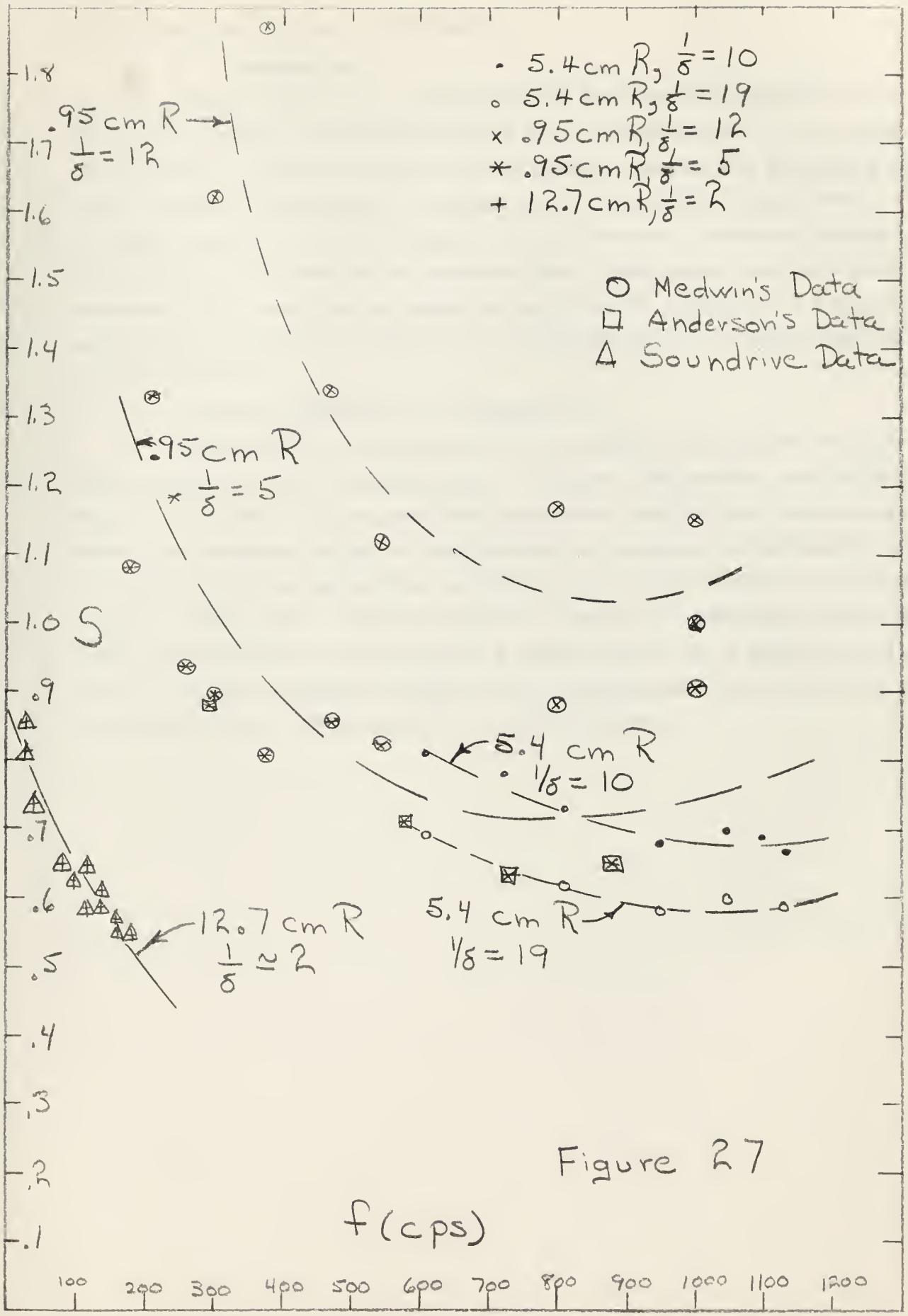
• 5.4cm R, 1/δ = 10
∘ 5.4cm R, 1/δ = 19
× .95cm R, 1/δ = 12
* .95cm R, 1/δ = 5
+ 12.7cm R, 1/δ = 2
O Medwin's Data
□ Anderson's Data
Δ Soundrive Data
.95 cm R
1/δ = 12
.95 cm R
* 1/δ = 5
5.4 cm R
• 1/δ = 10
5.4 cm R
1/δ = 19
12.7 cm R
1/δ ≃ 2
S
f (cps)
1.8
1.7
1.6
1.5
1.4
1.3
1.2
1.1
1.0
.9
.7
.6
.5
.4
.3
.2
.1
100
200
300
400
500
600
700
800
900
1000
1100
1200

Figure 27

VI. RECOMMENDED FURTHER INVESTIGATIONS

a. P_1 determination.

The determination of the effective pressure into which the successive shock waves are progressing has only been mentioned. It is apparent that the methods employed here cannot accurately measure the absolute pressures involved, consequently the value of P_1 could not be established. It was seen, however, that this pressure may be frequency dependent and undoubtedly is also dependent on pressure jump, temperature, and barometric pressure. This same type of investigation could be conducted at various ambient pressures and in a heated or cooled tube to get a greater indication of this dependence.

b. Frequency dependency of attenuation.

The effect of turbulence or tube radius on attenuation has only been suggested by this investigation. If higher frequencies could be generated in the same $1/\delta$ regions this dependence could be more adequately shown. An alternate method of determining the existence of turbulence and its distribution throughout the wave might be an optical study of the density patterns in the tube. The development of a method of generating finite amplitude pressure pulses other than by a siren, such as by a magnetostrictive device or a piston, should greatly extend the frequency range available and facilitate either or these methods of investigation.

VII. CONCLUSION

The four formulas describing the attenuation of acoustic shock waves have been compared with the data obtained in this investigation and that available from previous reports. In gathering the data contained in this report repeated similar runs were made at the same frequency and $1/\delta$ region in order to eliminate random fluctuations and errors as much as possible, and sets of runs were made at several different $1/\delta$ regions for each frequency. The $1/\delta$ region was varied by inserting attenuator pads of glass wool in the initial portion of the tube. Six different frequencies were run: 610, 725, 810, 950, 1050, and 1130 cps. All of the runs were made in a 5.4 cm radius steel tube under ambient atmospheric pressure and over a $1/\delta$ range of 8 to 35. The analysis made was based on the best 184 runs made.

A comprehensive analysis was made of the data, and available data obtained by previous investigators, both for frequency dependency and $1/\delta$ dependency. The experimental data supports Prof. Medwin's empirical formula in that S_w depends on the inverse of the frequency and our value of $S_\infty = .50$ is in agreement with Medwin's value of $S_\infty = .59$.

The unexplained dependence of S_w or $1/\delta$ was noted and an empirical formula was fitted to the data of this investigation.

Several collateral investigations are also reported on, including the influence of standing waves on attenuation, filters to match a tube to the source, wavelength measurements, propagation speed and temperature measurements, and attenuator pads for increasing the effective length of the tube.

It is believed that further studies of this phenomenon in air at atmospheric pressure should be made with different type of generating and measuring equipment, as significant improvement in the accuracy using present techniques would be difficult to achieve. Also the measurement of different gases and with different pressures requires different techniques.

VIII. BIBLIOGRAPHY

1. I. Rudnick, Report No. 42, Technical Report No. 1 on the High Amplitude Sound Abatement Research Program for the Office of Naval Research, Contract N8 onr 70502. Soundrive Engine Co., Los Angeles, Calif., 1952.

2. I. Rudnick, Report No. 48, Technical Report No. 3 on the High Amplitude Sound Abatement Research Program for the Office of Naval Research, Contract N8 onr 70502. Soundrive Engine Co., Los Angeles, California, 1953.

3. Report No. 49, Final Report on the High Amplitude Sound Abatement Research Program for the Office of Naval Research, Contract N8 onr 70502. Soundrive Engine Co., Los Angeles, Calif., 1953.

4. O.B. Wilson, Jr., and D.A. Bies, Report No. 79, Technical Note on Studies of Very High Amplitude Sound, Contract AF 18-600-495. Soundrive Engine Co., Los Angeles, Calif., 1954.

5. I. Rudnick, On the Attenuation of a Repeated Sawtooth Shock Wave, J. Acoust. Soc. Am. 25, 1012 (1953).

6. H. Medwin, H. Carpenter, R. Bauman, Attenuation of Repeated Plane Shock Waves in Air, Paper 7A6, Third International Congress on Acoustics, Germany, 1959.

7. G.C. Werth and L.P. Delsasso, Attenuation of Repeated Shock Waves in Tubes, J. Acoust. Soc. Am. 26, 59 (1954).

8. F.E. Fox and W.A. Wallace, Absorption of Finite Amplitude Sound Waves, J. Acoust. Soc. Am. 26, 994, (1954).

9. R.D. Fay, Plane Waves of Finite Amplitude, J. Acoust. Soc. Am. 3, 222 (1931).

10. R.D. Fay, Successful Method of Attack on Plane Progressive Finite Waves, J. Acoust. Soc. Am. 28, 910, (1956).

11. L.K. Zarembo, A Method for Determining the Width of the Front of an Acoustic Wave Similar in Form to a Sawtooth, Akusticheskii Zhurnal, 6, 43, (1960).

12. W.W. Lester, On the Theory of the Propagation of Plane, Finite Amplitude Waves in a Dissipative Fluid, J. Acoust. Soc. Am. 33, 1196 (1961).

13. J.H. Baltrukonis, Dynamics of a Hollow, Elastic Cylinder Contained by an Infinitely Long Rigid Circular-Cylindrical Tank, J. Acoust. Soc. Am. 32, 1539, (1960).

14. V. Timbrell, Generation of Weak Shock Waves, Nature 172, 540, (1953).

15. G.J. Barber and T.F. W. Embleton, Saw-Toothed Wave Forms in Sound, Nature 172, 1057, (1954).

16. L.R. Anderson and D.J. Mehrtens, Attenuation of Repeated Shock Waves in Tubes, Thesis, U.S. Naval Postgraduate School, Monterey, California, 1958.

17. H.L. Carpenter and R.W. Bauman, Attenuation of Repeated Shock Waves in Tubes, Thesis, U.S. Naval Postgraduate School, Monterey, California, 1959.

18. L.E. Kinsler and A.R. Frey, Fundamentals of Acoustics (John Wiley and Sons, Inc., New York, 1950).

19. L.E. Kinsler and A.R. Frey, Fundamentals of Acoustics, Draft Ch IX, (Unpublished).

20. H.W. Liepmann and A. Roshko, Elements of Gasdynamics (John Wiley and Sons, Inc., New York, 1957).

21. K. Osawatitsch, Gas Dynamics (Academic Press Inc., 1956).

22. P.J. Westervelt, 57th Meeting of the Acoustical Society of America, Paper L2, 15 May 1959.

23. D.T. Blackstock, Lagrangian One-Dimensional Equations of Hydrodynamics for a Viscous, Thermally Conducting Fluid, J. Acoust. Soc. Am. 33, 1245 (1961).

24. D.T. Blackstock, Propagation and Reflection of Plane Sound Waves of Finite Amplitude in Gases, Thesis, Harvard University, 1960.

25. D.C. Gazis, Three Dimensional Investigation of the Propagation of Waves in Hollow Circular Cylinders. I. Analytical Foundation, J. Acoust. Soc. Am. 31, 572, (1959).

IX. APPENDIX

a. Attenuation and Attenuators.

In order to increase the effective length of the tube, and thus the region of $1/\delta$ measured, two methods were employed. First, the pressure of the incoming compressed air was lowered so that smaller pulses were generated by the siren. This was found to be relatively ineffective, since lowering the pulse size also increased the distance for fully developed shock to form. The result was only a slight increase in the $1/\delta$ recorded at the far end of the tube, and a large reduction in the useable length of the tube.

The second method of obtaining high values of $1/\delta$ was to introduce an attenuator, pads of glass wool, in the tube at the junction of the 56" section and the main tube. This attenuator was found to attenuate the signal, as well as to leave the wave form almost unchanged. Thus, by putting in different numbers of pads and allowing a short distance downstream for the wave form to restabilize, the effective length of the tube could be extended to several times its actual length.

b. Wavelengh Measurements

The wavelength was determined in three independent ways. Excellent agreement was found among the different methods:

1. Standing wave measurements. By measuring the standing wave pattern on the recorder trace.

2. Direct measurement. By feeding the output from a traveling and a stationary microphone into a dual trace CRO and measuring directly the traveling microphone displacement between successive alignments.

3. Temperature. By utilizing a thermocouple placed about midway in the tube and projecting approximately 1" into the tube some average temperature for the air inside was determined. Using the perfect gas relation $c = c_o \sqrt{T/T_o}$, the speed of sound in the tube was calculated. This, divided by the frequency from the frequency counter, gives λ, assuming that the shock waves travel with the speed of sound at this temperature.

Agreement among the average of 8 or 9 standing wave measurements and the wavelength obtained by the other methods was generally to two significant figures, about the estimated accuracy of the measurements. The other two methods consistantly agreed, when the direct measurements were averaged over

8 or 9 wavelengths, to two significant figures, and usually to three. This also was consistant with the estimated accuracy of obtaining the measurements.

As the determination of λ by the direct measurement and temperature methods agreed so well, it was felt that the temperature used must be a characteristic of the shock waves.

When the siren was turned on, there was a rapid rise in temperature. After a few minutes, the rate of temperature rise became much slower. This rate seems to increase with increasing frequency. If the frequency is changed while the tube is running, a sudden change in temperature was noted before the new rate of rise was established. No correlation between the sign of this temperature change and the direction of frequency change was noted.

Since the true value of P_o is not known, a good approximation is to use the value of atmospheric pressure, which was done.

If there is to be no net dc flow of air through the tube, and none was noticed, the average pressure should be the barometric. It may be noted that there was 1/2" hole in the center of the base plate on the downstream end of the tube through which the microphone cables passed, so the tube was by no means air tight.

c. Standing Waves.

A short investigation of the effect of standing waves on attenuation in tubes was conducted at 1000 cps. A normal repeated shock wave was generated and its attenuation measured in the normal manner. Then a rubber diaphragm was placed in front of the termination to induce standing waves in the tube. Subsequently half and then three quarters of the diaphragm was cut away, in order to have standing waves of varying amplitude. The recorder traces of these different amplitude waves are shown in Fig. 28.

It was hoped that the measurement made on the standing waves might attenuate in the same manner as the incident shock waves and thus provide an alternate means of determining the attenuation of high $1/\delta$ shock waves that was free of noise, and independently check the values obtained by other means.

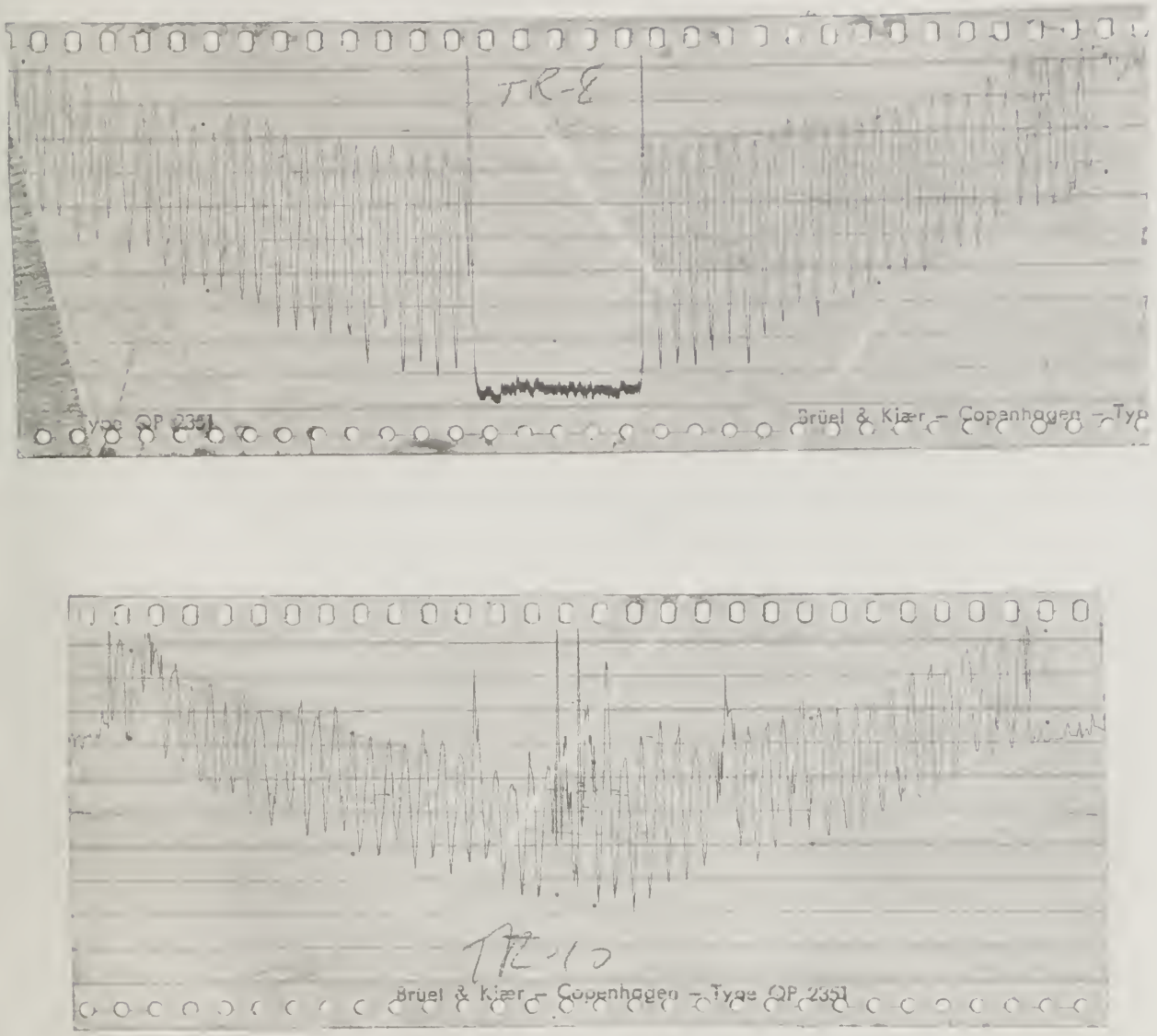

Figure 28. Standing waves of two amplitudes induced by partially obstructing termination with rubber diaphragm.

A careful analysis of the attenuation of the incident shock wave, whose value was obtained by averaging the standing wave envelope, showed that, apparently due to the non-linear action of the air, the S is smaller in a tube with a greater standing wave.

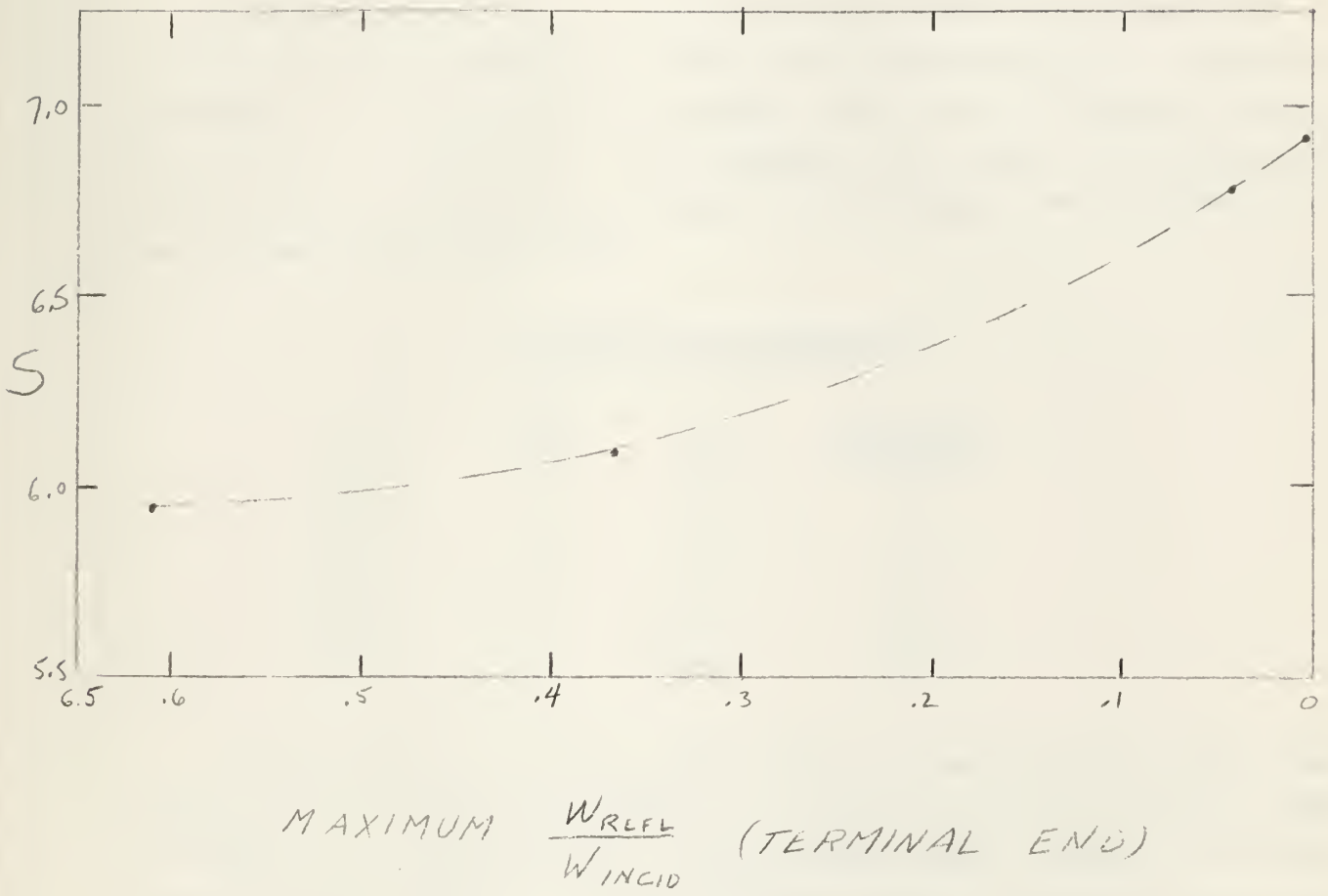

Fig. 29.

This averaging was made on the assumption that the peak values of the standing wave envelope represented the pressure jumps of the incident plus the reflected wave and the incident minus the reflected wave. Consequently the locus of the midpoints between successive peaks is the incident wave and

one half of the voltage between the top and bottom envelopes is the reflected wave. I.e.,

Top = Incident + Reflected

Bottom = Incident - Reflected

Incident = (top + bottom) 1/2

Reflected = (top - bottom) 1/2

A further analysis of the envelope of the standing wave showed that reflected it was attenuated at a greater rate than predicted for a repeated shock wave of the same pressure amplitude, both in the $1/\delta$ region of 12-25 and above 100. Consequently it was concluded that a study of the attenuation of the reflected waves would not extend the knowledge of the attenuation of the incident normal shock waves.

REFLECTED WAVE ATTENUATION

f	$1/\delta$	S	S(formula)
1000	15	.50	.64
1000	20	1.05	.67
1000	30	1.34	.74
1000	300	21.6	2.51
610	170	23.0	2.35

As the presence of standing waves would in no way help the study of the behavior of the normal incident waves, all further effort was directed toward the reduction of standing waves. The non-linear effects induced by the presence of standing waves of varying amplitudes could be of great interest, but their effects, per se , are outside the scope of the present study.

d. Filters.

In a preliminary investigation in a smaller diameter concentric tube, it was found that the extraneous noise level in the tube could be greatly reduced by the use of an acoustic style filter designed for a sound wave of equivalent wave length. The filter found to be most effective in matching

the different diameter tubes at the upstream end was designed as follows:

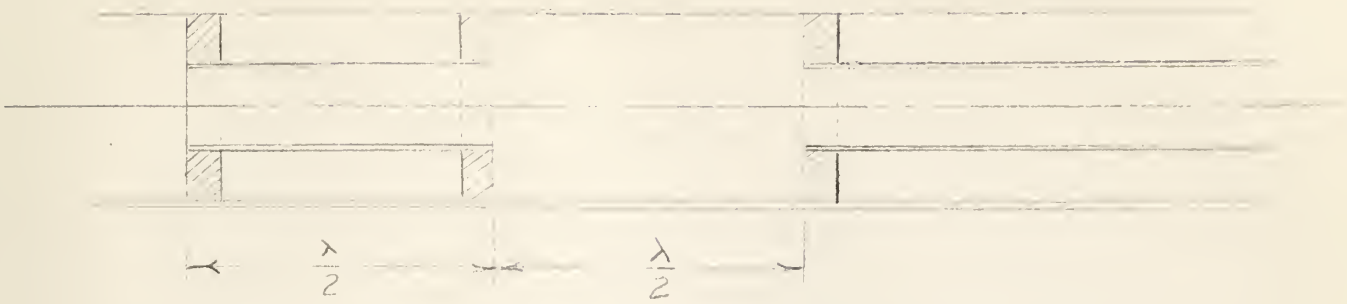

Fig. 30.

No method was found for matching the terminal end with a large sized termination that eliminated standing waves. The three types of intermediate connections tried were a filter like the upstream one, a stair-step $\lambda/2$ filter, and a long, slowly tapered cone.

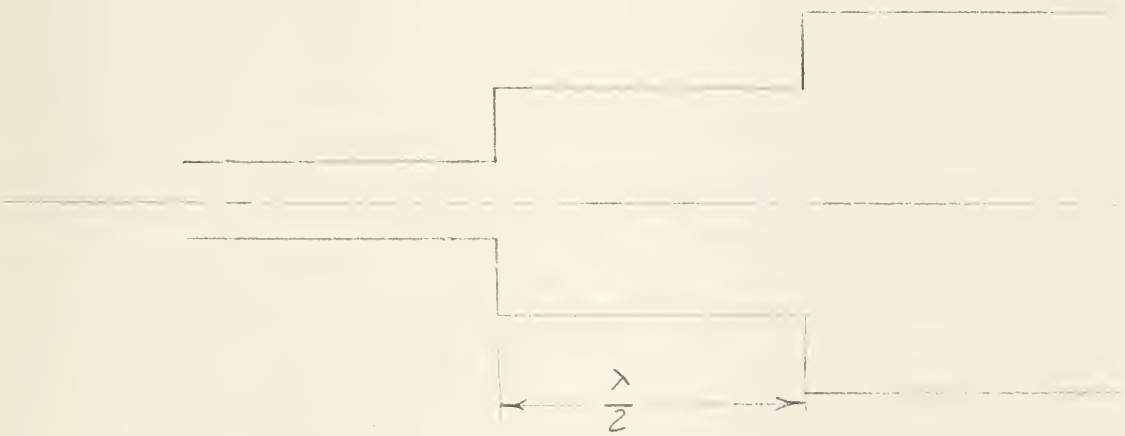

Fig. 31.

It was found to be much better to have a termination of the same diameter as the small tube rather then to try to match it to the better and more easily constructed large termination.